DOT-VNTSC-FAA-91-16

FAA Technical Center
Atlantic City, NJ 08405

Generation of Spectra and Stress Histories for Fatigue and Damage Tolerance Analysis of Fuselage Repairs

David Broek
FractuREsearch
and Samuel H. Smith
Richard C.Rice
Battelle
Columbus, Ohio 43201

Final Report
October 1991

This document is available to the public through the National Technical Information Service Springfield, Virginia 22161

U.S. Department of Transportation
Federal Aviation Administration

Technical Report Documentation Page

1. Report No.	2. Government Accession No.	3. Recipient's Catalog No.
4. Title and Subtitle Generation of Spectra and Stress Histories for Fatigue and Damage Tolerance Analysis of Fuselage Repairs		5. Report Date October 1991 6. Performing Organization Code DTS-71
7. Author(s) D. Broek, S.H. Smith, R.C. Rice		8. Performing Organization Report No. DOT-VNTSC-FAA-91-
9. Performing Organization Name and Address Battelle* 505 King Avenue Columbus, OH 43201-2693		10. Work Unit No. (TRAIS) FA1D8/A1061 11. Contract or Grant No. DTRS-57-89-C-00006
12. Sponsoring Agency Name and Address U.S. Department of Transportation Federal Aviation Administration Technical Center Atlantic City, NJ		13. Type of Report and Period Covered Final Report March 1990 - May 1991 14. Sponsoring Agency Code ACD-210

15. Supplementary Notes

*Under contract to: U.S. Department of Transportation
Research and Special Programs Administration
Volpe National Transportation Systems Center
Cambridge, MA 02142-1093

16. Abstract

This report describes a simplified procedure for the development of stress histories for use in the analysis of aircraft repairs. Although repairs of all components of the airframe are of interest, this report concentrates on stress histories for fuselage skin repairs. A description of typical fuselage loadings is provided, and basic fuselage stress histories are described. A method for development of an exceedance diagram for analysis of fuselage skin repairs is detailed. Subsequently, a methodology for generating detailed stress histories is reviewed. Some of the key features are 1) the inclusion of a range of flights of different severities, 2) the inclusion of deterministic loads where they occur, e.g., ground-air-ground cycles, 3) the use of a near-optimum number of stress levels (10-16 positive and negative), 4) the combination of positive and negative excursions of equal frequency, and 5) matching of the total number of flights and cycles with the total exceedance diagram. Two methods of estimating fuselage skin stresses are presented, the first based on static equilibrium requirements and the second based on a limit load analysis.

A comparison of the proposed history generation scheme with that of an airframe manufacturer for the KC-135 is also presented. The predicted fatigue crack growth patterns for a hypothetical through crack at a fastener hole are compared for the two history generation schemes at three areas within a fuselage. Predicted crack growth lives are within a factor of 1.5 for two of the three cases. For the third case (which is predicted to be the least severe by both techniques), the proposed scheme results in substantially longer crack growth life predictions. The probable reasons for these differences are discussed.

17. Key Words	18. Distribution Statement
Aircraft, Fuselage Repairs, Spectra, Stress Histories, Stress Analysis Damage Tolerance, Fatigue	DOCUMENT IS AVAILABLE TO THE PUBLIC THROUGH THE NATIONAL TECHNICAL INFORMATION SERVICE, SPRINGFIELD, VA 22161

19. Security Classification (of this report)	20. Security Classification (of this page)	21. No. of Pages	22. Price
UNCLASSIFIED	UNCLASSIFIED	46	

Form DOT F 1700.7 (8/72) Reproduction of this completed page authorized

METRIC / ENGLISH CONVERSION FACTORS

ENGLISH TO METRIC

LENGTH (APPROXIMATE)

1 inch (in) = 2.5 centimeters (cm)
1 foot (ft) = 30 centimeters (cm)
1 yard (yd) = 0.9 meter (m)
1 mile (mi) = 1.6 kilometers (km)

AREA (APPROXIMATE)

1 square inch (sq in, in^2) = 6.5 square centimeters (cm^2)
1 square foot (sq ft, ft^2) = 0.09 square meter (m^2)
1 square yard (sq yd, yd^2) = 0.8 square meter (m^2)
1 square mile (sq mi, mi^2) = 2.6 square kilometers (km^2)
1 acre = 0.4 hectares (he) = 4,000 square meters (m^2)

MASS - WEIGHT (APPROXIMATE)

1 ounce (oz) = 28 grams (gr)
1 pound (lb) = .45 kilogram (kg)
1 short ton = 2,000 pounds (lb) = 0.9 tonne (t)

VOLUME (APPROXIMATE)

1 teaspoon (tsp) = 5 milliliters (ml)
1 tablespoon (tbsp) = 15 milliliters (ml)
1 fluid ounce (fl oz) = 30 milliliters (ml)
1 cup (c) = 0.24 liter (l)
1 pint (pt) = 0.47 liter (l)
1 quart (qt) = 0.96 liter (l)
1 gallon (gal) = 3.8 liters (l)
1 cubic foot (cu ft, ft^3) = 0.03 cubic meter (m^3)
1 cubic yard (cu yd, yd^3) = 0.76 cubic meter (m^3)

TEMPERATURE (EXACT)

$[(x - 32)(5/9)]$ °F = y °C

METRIC TO ENGLISH

LENGTH (APPROXIMATE)

1 millimeter (mm) = 0.04 inch (in)
1 centimeter (cm) = 0.4 inch (in)
1 meter (m) = 3.3 feet (ft)
1 meter (m) = 1.1 yards (yd)
1 kilometer (km) = 0.6 mile (mi)

AREA (APPROXIMATE)

1 square centimeter (cm^2) = 0.16 square inch (sq in, in^2)
1 square meter (m^2) = 1.2 square yards (sq yd, yd^2)
1 square kilometer (km^2) = 0.4 square mile (sq mi, mi^2)
1 hectare (he) = 10,000 square meters (m^2) = 2.5 acres

MASS - WEIGHT (APPROXIMATE)

1 gram (gr) = 0.036 ounce (oz)
1 kilogram (kg) = 2.2 pounds (lb)
1 tonne (t) = 1,000 kilograms (kg) = 1.1 short tons

VOLUME (APPROXIMATE)

1 milliliter (ml) = 0.03 fluid ounce (fl oz)
1 liter (l) = 2.1 pints (pt)
1 liter (l) = 1.06 quarts (qt)
1 liter (l) = 0.26 gallon (gal)
1 cubic meter (m^3) = 36 cubic feet (cu ft, ft^3)
1 cubic meter (m^3) = 1.3 cubic yards (cu yd, yd^3)

TEMPERATURE (EXACT)

$[(9/5)y + 32]$ °C = x °F

QUICK INCH-CENTIMETER LENGTH CONVERSION

INCHES	0	1	2	3	4	5	6	7	8	9	10

CENTIMETERS 0 1 2 3 4 5 6 7 8 9 10 11 12 13 14 15 16 17 18 19 20 21 22 23 24 25 | 25.40

QUICK FAHRENHEIT-CELCIUS TEMPERATURE CONVERSION

°F	-40°	-22°	-4°	14°	32°	50°	68°	86°	104°	122°	140°	158°	176°	194°	212°
°C	-40°	-30°	-20°	-10°	0°	10°	20°	30°	40°	50°	60°	70°	80°	90°	100°

For more exact and or other conversion factors, see NBS Miscellaneous Publication 286, Units of Weights and Measures. Price $2.50. SD Catalog No. C13 10 286.

Preface

Work reported in this document was accomplished under the direction of the Volpe National Transportation Systems Center (VNTSC), Cambridge, Massachusetts and the sponsorship of the Federal Aviation Administration Technical Center, Atlantic City, New Jersey. Dr. John Brewer is the current VNTSC technical task initiator for this effort, which was conducted as Subtask 4 on TTD No. VA-0013 under Contract No. DTRS-57-89-C-00006.

This report describes a simplified procedure for the development of stress histories for use in the analysis of aircraft fuselage repairs. The work was performed by Dr. David Broek of FractuResearch in conjunction with Messrs. Richard Rice and Samuel Smith of Battelle.

The authors acknowledge the support of Melanie Violette, formerly of the VNTSC, on this task. In addition, we acknowledge the efforts of the following reviewers — Mr. Tom Swift, Los Angeles Aircraft Certification Office FAA, Long Beach, California; Dr. Jack Lincoln, ASD/ENFS, Wright Patterson AFB, Ohio; and Mr. Tom Disney, Marietta, Georgia.

Table of Contents

List of Figures

List of Abbreviations

AWACS	Airborne Warning and Control System
DOT	Department of Transportation
DT	Damage Tolerance
FAA	Federal Aviation Administration
GAG	Ground-air-ground
NASA	National Aeronautics and Space Administration
OEM	Original Equipment Manufacturer
TWIST	Standardized Spectrum for Transport Aircraft Wing Structures
VGH	Velocity, Acceleration and Altitude

List of Symbols

$\overline{A}$, $\overline{A}$	Parameters, dependent on aircraft type
A_{st}	Area of tear strap
C	Coefficient
cg	Center of gravity
C_L	Three dimensional lift coefficient
$dC_L/d\alpha$	Slope of C_L vs. α curve
g, G	Acceleration of gravity
G_{al}	Gust alleviation factor
k	Number of stringers
L	Lift load (force)
m	Mass
M_b	Bending moment
M_t	Torsional moment
n_z	Vertical acceleration load factor
N	Number of cycles
p	Pressure level
r	Radius of curvature
R	Fuselage radius
S	Wing area
t	Fuselage skin thickness
T	Tail load (force)
v	Gust velocity
V	Airspeed
V_t	Density of air
w	Angular velocity

List of Symbols (Continued)

W	Weight
z	Z-direction distance
α	Angle of attack
α_1	Constant dependent on stiffening ratio
$\Delta\alpha$	Increment of α
$\Delta\sigma_{bl}$	Range of bending stress
ΔL	Incremental lift
ρ	Density of air
σ_1	Cyclic stress
σ_{bl}	Bending stress
σ_{bl-1g}	1g bending stress
σ_{LL}	Limit load stress
σ_m	Mean stress
σ_{max}	Maximum stress
σ_p	Circumferential pressurization stress (hoop stress)
σ_{pl}	Longitudinal pressurization stress
σ, σ_t	Total stress
σ_{1g}	One g stationary stress
τ_t	Shear stress
θ	Angle of vector

Executive Summary

This report describes a simplified procedure for the development of stress histories for use in the analysis of aircraft repairs. Although repairs of all components of the airframe are of interest, this report concentrates on stress histories for fuselage skin repairs. A description of typical fuselage loadings is provided, and basic fuselage stress histories are described. A method for development of an exceedance diagram for analysis of fuselage skin repairs is detailed. A methodology for generating detailed stress histories is also reviewed.

Some of the key features of this methodology are (1) the inclusion of a range of flights of different severities, (2) the inclusion of deterministic loads where they occur, e.g. ground-air-ground cycles, (3) the use of a near-optimum number of stress levels (10-16 positive and negative), (4) the combination of positive and negative excursions of equal frequency, and (5) matching of the total number of flights and cycles with the total exceedance diagram. Two methods of estimating fuselage skin stresses are presented, the first based on static equilibrium requirements and the second based on a limit load analysis.

A comparison of the proposed history generation scheme with that of an airframe manufacturer for the KC-135 is also presented. The predicted fatigue crack growth patterns for a hypothetical through crack at a fastener hole are compared for the two history generation schemes at three areas within a fuselage. Predicted crack growth lives are within a factor of 1.5 for two of the three cases. For the third case (which is predicted to be the least severe by both techniques) the proposed scheme results in substantially longer crack growth life predictions. The probable reasons for these differences are discussed.

1. INTRODUCTION

Commercial aircraft operators are required by FAA regulations to repair damaged aircraft structure. This must be performed in a timely manner so that the aircraft downtime is kept to a minimum and the loss of revenue is small. In many instances the airline operator will not have enough time to obtain structural repair data, analysis or information from the original equipment manufacture (OEM) and needs to perform the fatigue and damage tolerance (DT) analysis of the repair himself using simple straightforward analytical tools and the OEM repair manuals.

The FAA aging aircraft program has many programs and tasks directed at enhancing the engineering evaluation of the structural integrity of aircraft repairs. In general the guiding principle for an aircraft structural repair is to restore the structure to its original (or better) static strength and stiffness capability. However, the repair must also be designed for adequate fatigue resistance, damage tolerance and inspectability.

Fatigue and DT analyses must be based on realistic stress histories, which, in turn, must be derived from realistic load spectra. Therefore, an algorithm for the development of a stress history must be included in an analysis of repairs. This report describes a simple and straightforward method to obtain an approximate stress history for specific locations in an aircraft fuselage.

It is important to recognize that the structural analysis and stress spectrum loadings development described here are approximate analyses and have certain limitations. The results can be used to compare the quality of different repair options or to compare the quality of a candidate repair with the original structure. If more precise and quantitative analyses are required, more detailed structural analysis and stress results for specific locations in the aircraft should either be obtained from the OEM or calculated through the use of sophisticated structural analysis codes such as finite element methods.

Although repairs of all components of the airframe are of interest, this report concentrates on stress histories for fuselage skin repairs. For other cases this basic approach can be generalized for wings and empennages with limited additional effort.

This report first considers fuselage loading in Section 2. A realistic spectrum is derived in Section 3, and the algorithm for stress history generation follows in Section 4. Section 5 briefly addresses ways to obtain estimates of actual fuselage stresses[1]. Finally, Section 6 offers a comparison of the proposed stress history generation scheme with that used by an aircraft manufacturer.

2. FUSELAGE LOADING

2.0 Loading Segments

An aircraft fuselage is subjected to flight segments with different loading content during a typical flight. The loading consists of the 1.0 g stationary load and dynamically induced loadings. The flight segments within which the dynamic loading occurs are taxiing and take-off, ascent/climb with pressurization, cruise, descent with depressurization, landing impact and taxiing. Over the years NASA and the FAA have conducted several flight loading surveys on the response of commercial aircraft to gust and maneuver loadings. The experimental data taken in the form of velocity, g-levels and altitude (VGH) are reduced to basic exceedance curves for the various types of aircraft such as large or medium size and commuter aircraft. The cyclic content and magnitude of stresses at a particular fuselage location are determined from exceedance diagrams for gust and maneuver loadings. Reference [2] provides detailed data on the most recent NASA/DOT/FAA program on VGH flight loadings data for the B727, L-1011, DC10, and B747 aircraft.

The stress history development for a given location in the fuselage must consider the pressurization, gust and maneuver loadings. The primary loadings in the fuselage are the pressure loads with superimposed maneuver and gust loadings. The stresses at the location selected for an analysis are determined by structural load transfer functions which account for the response of the aircraft fuselage to gusts and maneuvers. The determination of pressurization stresses is straightforward.

2.1 Gust Loadings

The normal coordinate system for the aircraft structure is shown in Figure 1. Besides pressurization, the next primary source of cyclic loading on a commercial aircraft fuselage is gust. Gust loads on the wing will cause cyclic fuselage bending; lateral gusts on the tail fin will cause fuselage torsion. As such, the gust spectrum is relevant to the definition of fuselage cyclic loads. Figure 2 explains the elements of gust loading. During normal stationary flight the lift is equal to the aircraft's weight ($L = W$), regardless of altitude, airspeed or angle of incidence, each of these being appropriately adjusted according to circumstances. Note that the tail load, T, is generally small (positive or negative) and ideally equal to zero. The tail is needed only to equilibrate the total moment and to account for maneuvers.

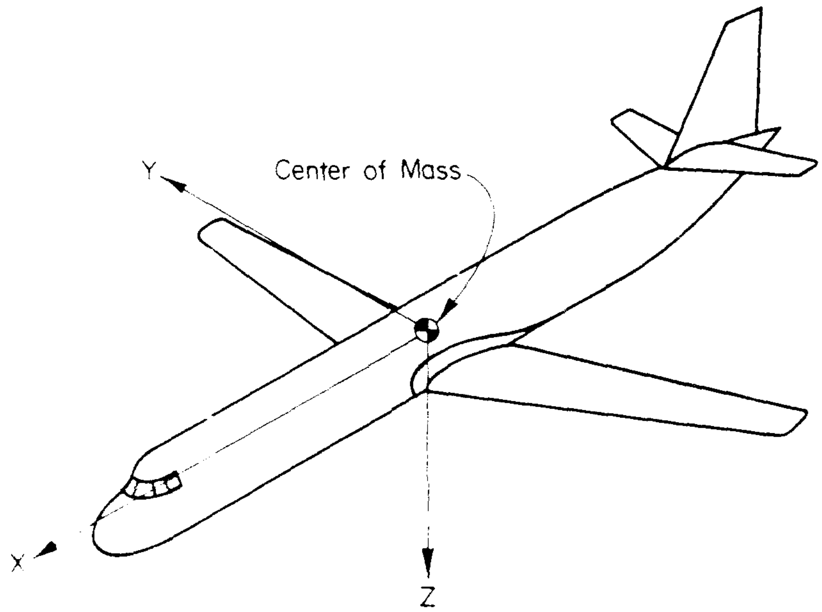

FIGURE 1. COORDINATE SYSTEM

A gust causes a ΔL up or down, as shown in Figure 2c. For a ramp-type or *(1-cosine)* gust, a gust alleviation factor, G_{al}, must be included, which depends upon aerodynamic inertia. A large, sluggish aircraft (747 or DC10) has a lower G_{al} than a smaller one (737 or DC9). Equation (1) shows that for a particular aircraft type the ΔL is always proportional to the gust velocity, U, and the airspeed, V, regardless of altitude.

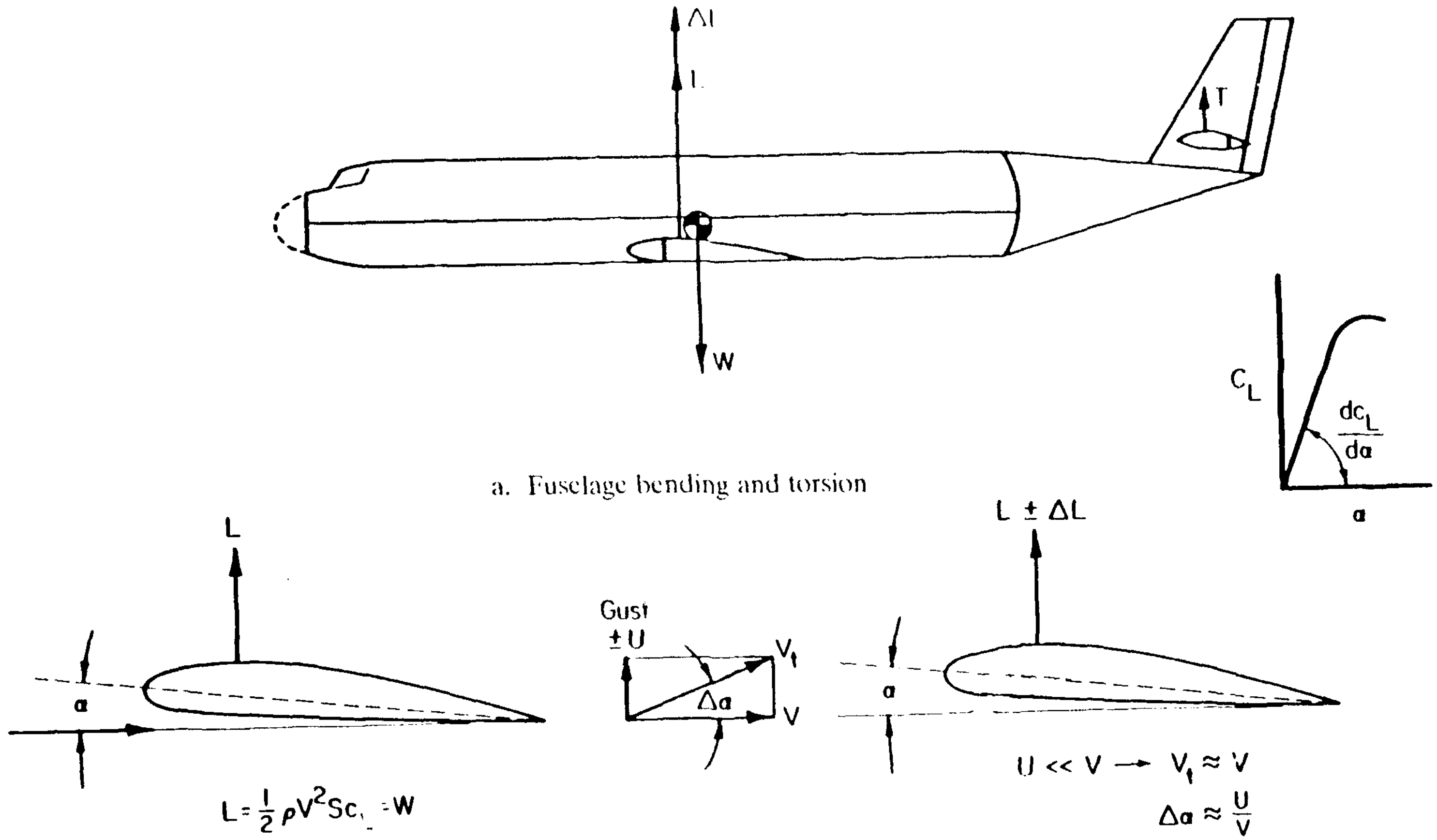

a. Fuselage bending and torsion

b. Stationary flight

c. Gust

FIGURE 2. GUST LOADING ΔL

$$
\begin{aligned}
\Delta L &= \frac{1}{2}\,\rho V^2 S\ G_{al}\,\frac{dC_L}{d\alpha}\,\Delta\alpha \\
&= \frac{1}{2}\,\rho V^2 S\ G_{al}\,\frac{dC_L}{d\alpha}\,\frac{U}{V} \qquad (1)\\
&= \frac{1}{2}\,\rho S\ G_{al}\,\frac{dC_L}{d\alpha}\,UV \approx C\ UV
\end{aligned}
$$

where

ρ = Density of the air
S = Wing area
G_{al} = Gust alleviation factor depending on aircraft and altitude
C_L = Three dimensional lift coefficient
α = Angle of attack, angle between free-stream and wing velocity and wing chord line
$\frac{dC_L}{d\alpha}$ = Slope of C_L vs. α curve
C = 1/2 product of above factors.

Substituting L (with $L = W$), one can also derive Equations (2a) and (2b), where $\bar{A}$ and $\bar{\bar{A}}$ depend upon the aircraft type.

$$\Delta L = L\ G_{al}\,\frac{dC_L}{d\alpha}\,\frac{1}{C_L}\,\frac{U}{V} = \bar{\bar{A}}\ W\,\frac{U}{V} = \bar{A}\ WU \qquad (2a)$$

$$n_z = \frac{L + \Delta L}{L} = \frac{W + \Delta L}{W} = \frac{W + \bar{A}WU}{W} = 1 + \bar{A}\ U \qquad (2b)$$

Note that most airliners basically fly at the same average airspeed. This leads to the equation for vertical acceleration, n_z, as in Equation (2b). Hence, the bending moment, and, therefore the cyclic stress (per Equation (3)), is proportional to U, where C depends upon the aircraft type weight distribution and fuel load.

$$\sigma = \sigma_{1g} \pm C\sigma_{1g} \tag{3}$$

It follows that fuselage cyclic loading can be derived directly from gust spectra, especially wing spectra, as shown in Sections 3-5.

2.2 Maneuvers

Cyclic loads due to maneuvers are a consequence of inertia forces. As shown for two typical maneuvers in Figures 3 and 4, the center of gravity (c.g.) acceleration, n_z, can be determined for any maneuver. Although maneuvers are the primary source of cyclic loads for fighters and trainers, for commercial aircraft, maneuver loads are small and infrequent compared to gust loads.

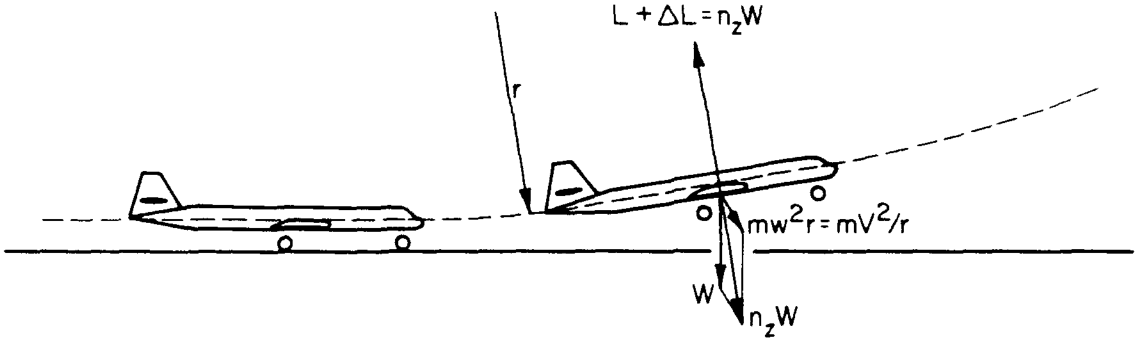

FIGURE 3. MANEUVER LOADING TAKE-OFF ROLL

2.3 Basic Fuselage Stress History

Gust and maneuver loads are not the only source of cyclic stress on a fuselage. The pressurization cycle, occurring once per flight, is a major contributor, especially for circumferential stresses. Table 1 provides a summary of typical pressurization stresses for common commercial aircraft. Combination of the appropriate pressurization stresses with the gust and maneuver induced stresses discussed in Sections 2.1 and 2.2 leads to the stress histories shown in Figure 5.

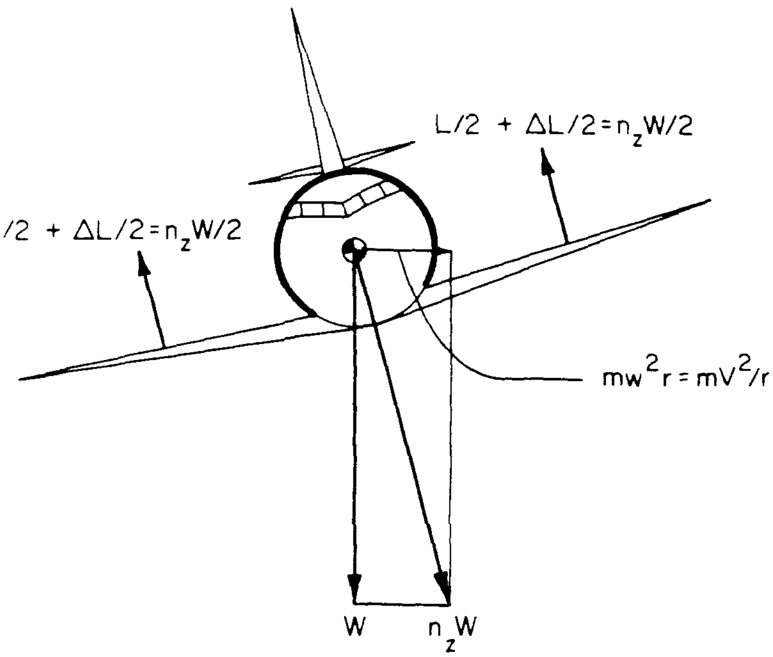

FIGURE 4. MANEUVER LOADING BANKING IN CURVE

For circumferential stresses, the hoop stress, σ_p, is the basic flight-by-flight cycle, essentially the ground-air-ground (GAG) cycle. Longitudinal stresses for the stationary flight have two contributors, one due to pressurization (roughly half the hoop stress) and one due to fuselage bending, following from the 'normal' weight distribution in the fuselage. Thus the GAG cycle consists of two superimposed components, as shown in Figure 5b.

Cyclic stresses due to bending by inertia forces from vertical gusts and maneuvers are superimposed on the GAG cycle. Torsional loadings are generally small and have a zero mean because fin loads are normally zero. However, cyclic torsional stresses do occur due to lateral gusts and maneuvers.

TABLE 1. VARIATION IN AIRCRAFT HOOP STRESSES

Hoop Stress, ksi	Aircraft	Alloy	Minimum Skin Thickness, inches
9.8	DC9	2014/24-T6	0.050
12.8	DC-8	2014-T6	0.050
14.8	L-1011	7075-T76	0.068
15.0	DC-10	2024-T3	0.068
15.7	737	2024-T3/T4	0.036
15.9	707/727	2024-T3/T4	0.040
18.3	747	2024-T3	0.063

3. THE EXCEEDANCE DIAGRAM

3.1 Measured Spectra and the TWIST Standard

As demonstrated in Section 2, and especially in Figure 5, the major fuselage cycle is the GAG cycle due to internal pressurization; the superimposed cyclic stresses are due primarily to the fuselage response to the wing, which is subjected to gust and maneuver loadings. The fuselage stresses are due to inertia loads, which in turn are due to wing loads. Thus, the fuselage spectrum for the bending loads can be obtained from the wing spectrum using the proper load-to-stress conversions (stress transfer functions) obtained from structural analyses.

The best way to obtain the cyclic stress spectrum due to gusts and maneuvers is from measurements. Extensive measurements on wings were made[2,3]; they are shown in Figure 6 (many more are presently available). Obviously, different aircraft types have somewhat different spectra, which is mainly due to the difference in the gust alleviation factor G_{al}, or α and C, the parameters shown in Equations (1) and (2). Also note that these measured spectra inherently include maneuver loads. The latter are small compared with the gust loads. The spectra are essentially symmetric and nearly linear on a semi logarithmic scale.

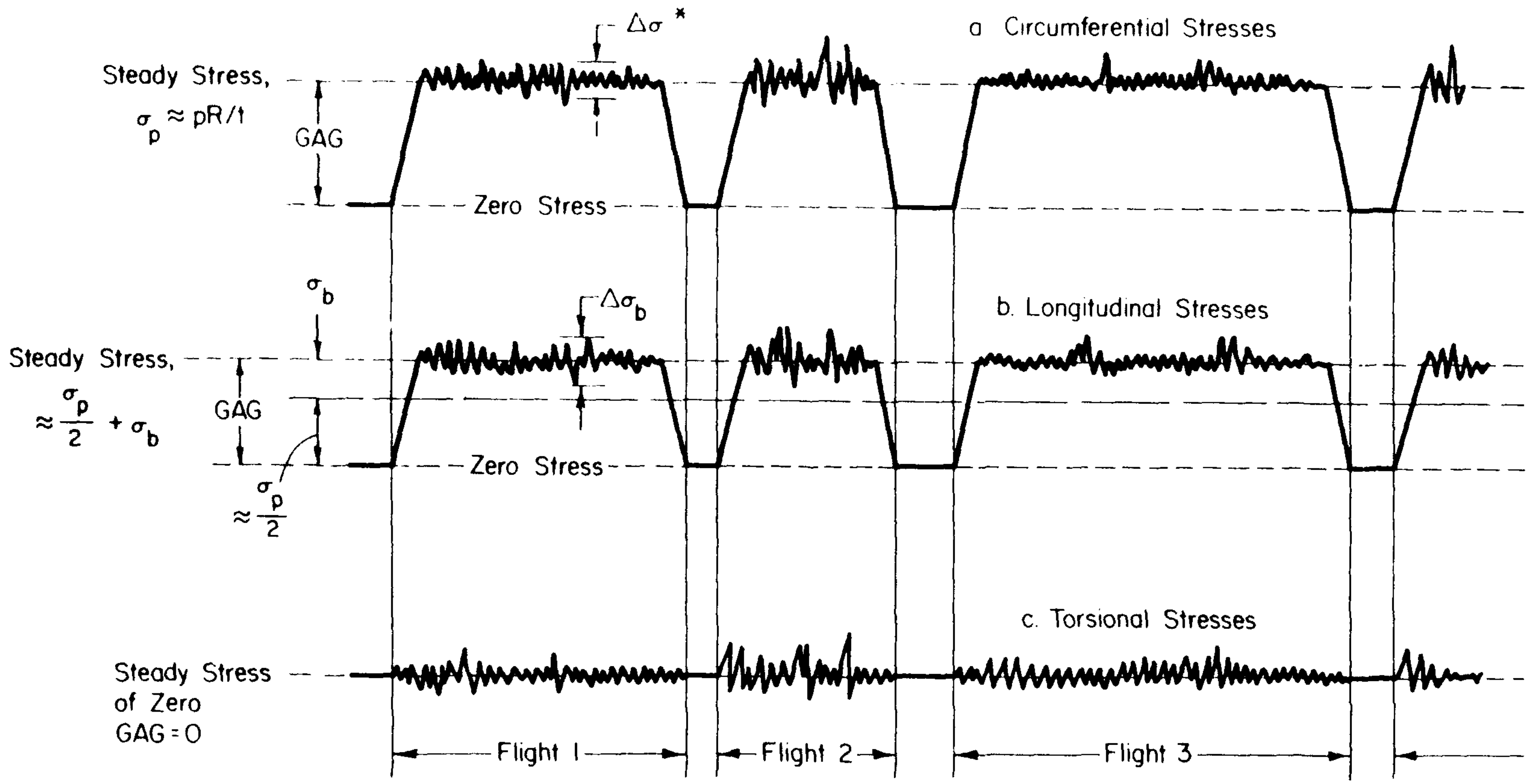

* $\Delta\sigma$ due to bending + torsion

FIGURE 5. TYPICAL STRESS HISTORIES FOR AIRCRAFT FUSELAGE

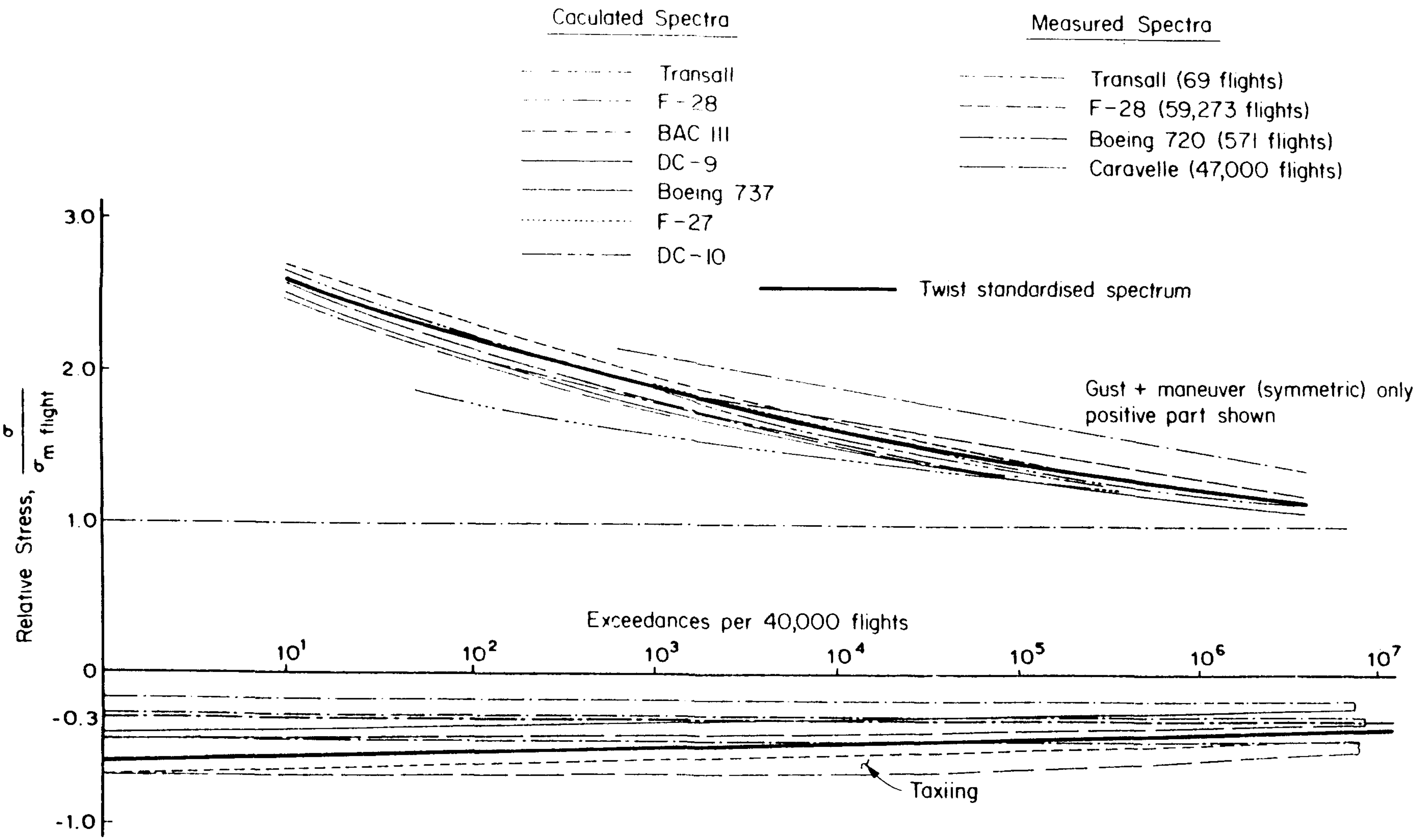

FIGURE 6. LOAD SPECTRA PERTAINING TO 40,000 FLIGHTS FOR DIFFERENT AIRCRAFT

These measured spectra were used[3] to establish a standard spectrum, called TWIST, which is also shown in Figure 6 and in more detail in Figure 7. Note that the stresses are expressed as a ratio to the 1g stationary flight stress, so that adjustments can be made for the stress level: the stress axis can be obtained when the 1g stress level is known. It should be pointed out that TWIST was developed for comparative testing. It is *not* a standard spectrum *for design*. Nevertheless, it can serve very well as a basis for the present purpose *provided* the stress levels are adjusted for fuselages of different aircraft systems.

Since TWIST is used for testing, detailed procedures have been developed to generate stress histories from the exceedance diagram of Figure 6. Although such histories are useful for testing, they are cumbersome, to say the least, for analysis; easier, but similar ways to derive stress histories can be devised, as will be shown in Section 4.

3.2 Proposed Spectrum

The TWIST exceedance diagram is repeated in Figure 8, together with a proposed simplification. The simplification is not essential; the TWIST exceedance diagram could be used as is. However, since it is an average, some streamlining is justified, especially since the stress axis must be adjusted for different fuselages types (Section 5).

TWIST is a spectrum for 40,000 flights of an estimated average duration of 1.5 hours; hence it is a spectrum for about 60,000 hours, the normal aircraft design life. In the case of fuselages for aircraft with largely different flight durations, the GAG cycle occurs more or less frequently. As the GAG cycle is of major importance (Figure 5), the spectrum must be considered to be for 60,000 hours instead of for 40,000 flights. This is perfectly legitimate, because the number of gusts per hour is of more importance than the number of gusts per flight.

The TWIST spectrum ends at a minimum of 10 exceedances. This essentially means that it is clipped at 10 exceedances per 60,000 hours. Clipping and truncation of the spectrum is of no consequence if crack growth retardation due to overloads is not accounted for in the fatigue crack growth analysis of the repair [1]. However, it is of great importance if retardation is to be considered [1,4,5]. Performing linear crack growth analysis without consideration for retardation effects is generally conservative.

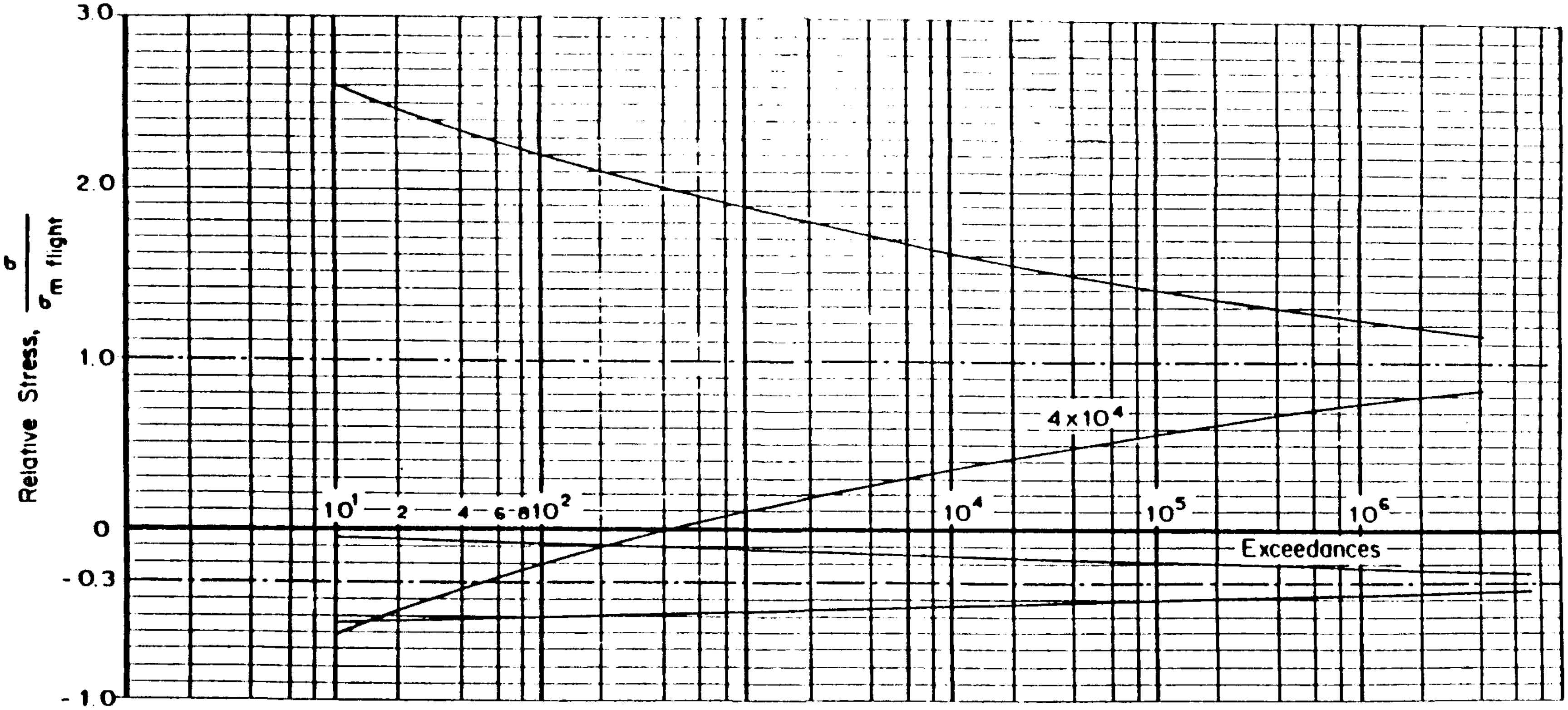

FIGURE 7. STANDARDIZED SPECTRUM FOR 40,000 FLIGHTS TWIST

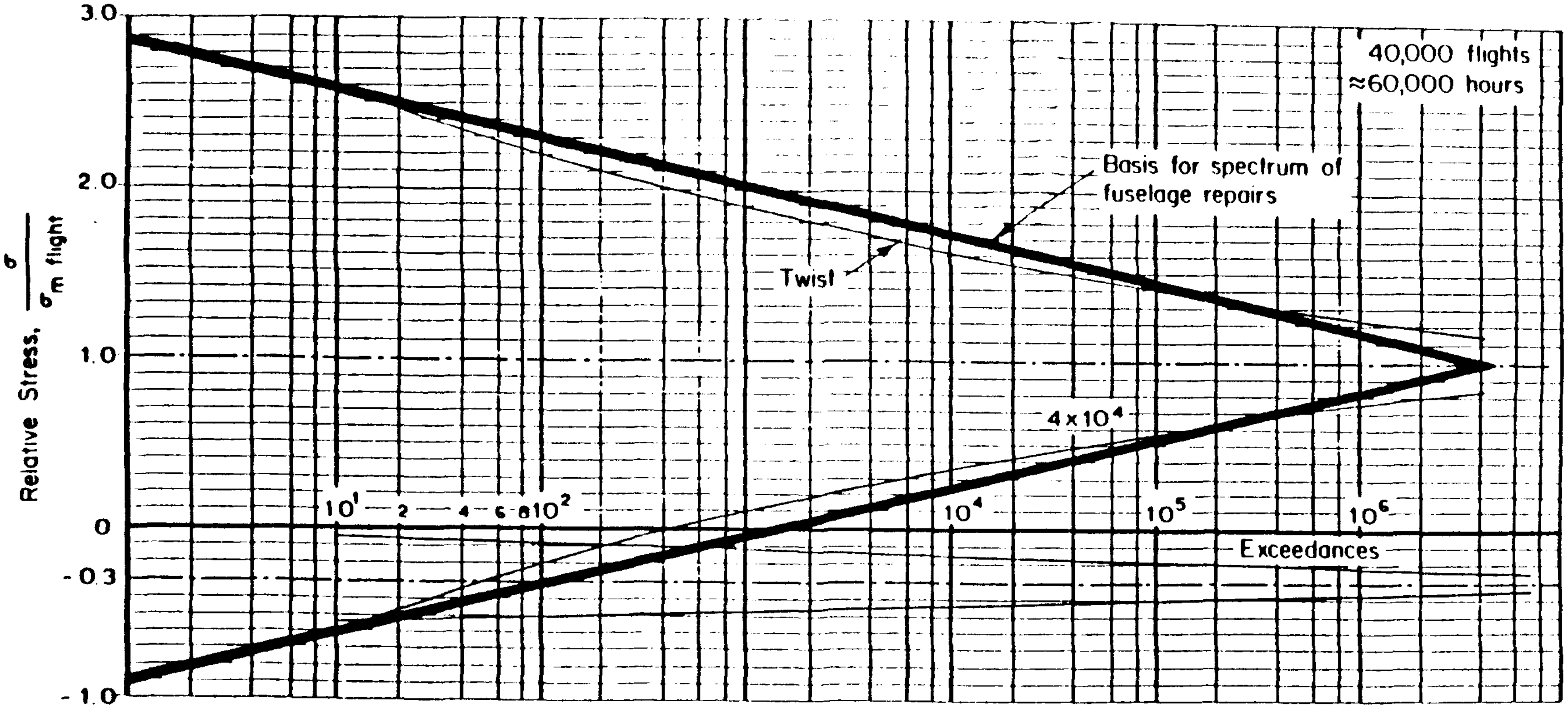

FIGURE 8. PROPOSED SIMPLIFICATION TO STANDARDIZED TWIST SPECTRUM FOR 40,000 FLIGHTS

As discussed in Section 4, a 60,000 hour spectrum is unwieldy and unnecessary for stress history generation, especially when it is clipped anyway. Therefore, the proposed spectrum is reduced to one for 600 hours. The logic for the reduction can be understood by comparing Figures 9 and 10. The 600 hour spectrum of Figure 10 is same as the one in Figures 8 and 9, but is more suitable for the stress history generation explained in Section 4. Note that this spectrum is "automatically" clipped at the once per 600 hours exceedance (100 times per 60,000 hours), which is more conservative if retardation is accounted for [1] and [4]. The spectrum shown in Figure 10 can be converted to stress quite easily, since the fuselage pressurization stress and the limit load stress are known for all certified aircraft. This will be explained in Section 5.

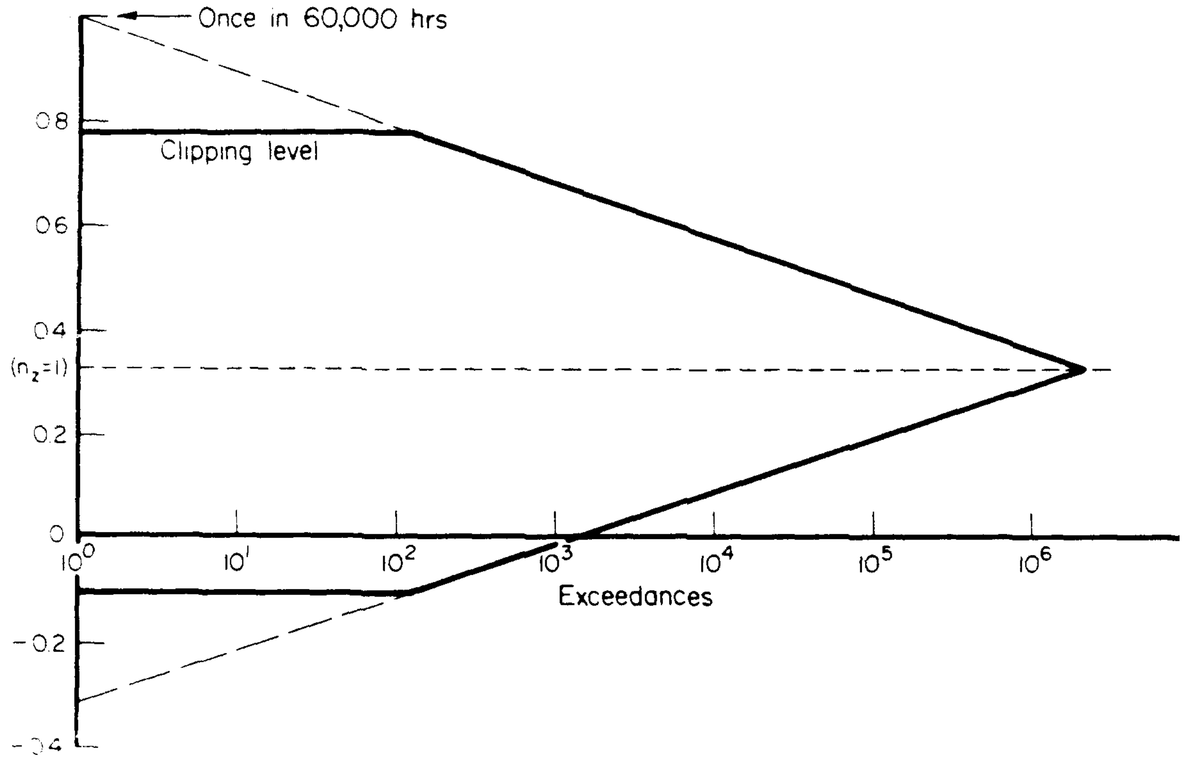

FIGURE 9. REPAIR SPECTRUM (SEE FIGURE 8) IN TERMS OF n_z

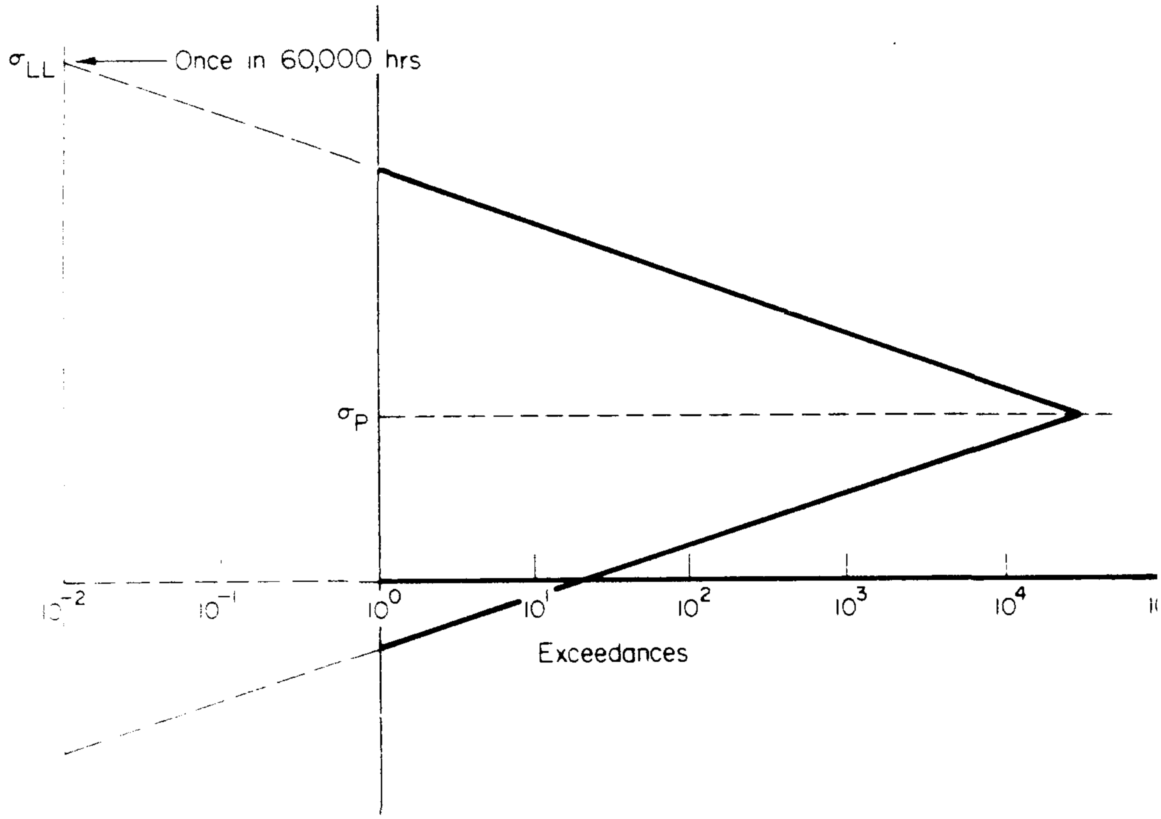

FIGURE 10. REPAIR SPECTRUM FOR 600 HRS (COMPARE TO FIGURE 9)

4. STRESS HISTORY GENERATION

4.1 Stress Levels

Depending upon the counting procedure, the exceedance diagram shows the number of times a positive or negative stress excursion is exceeded; i.e., it shows the size of the stress range and their frequency. In the schematic example in Figure 11, stress Level 4 is exceeded 3,000 times and Level 3 is exceeded 20,000 times. As a result, there will be 20,000 - 3,000 = 17,000 events in which the stress reaches a level somewhere between Levels 3 and 4.

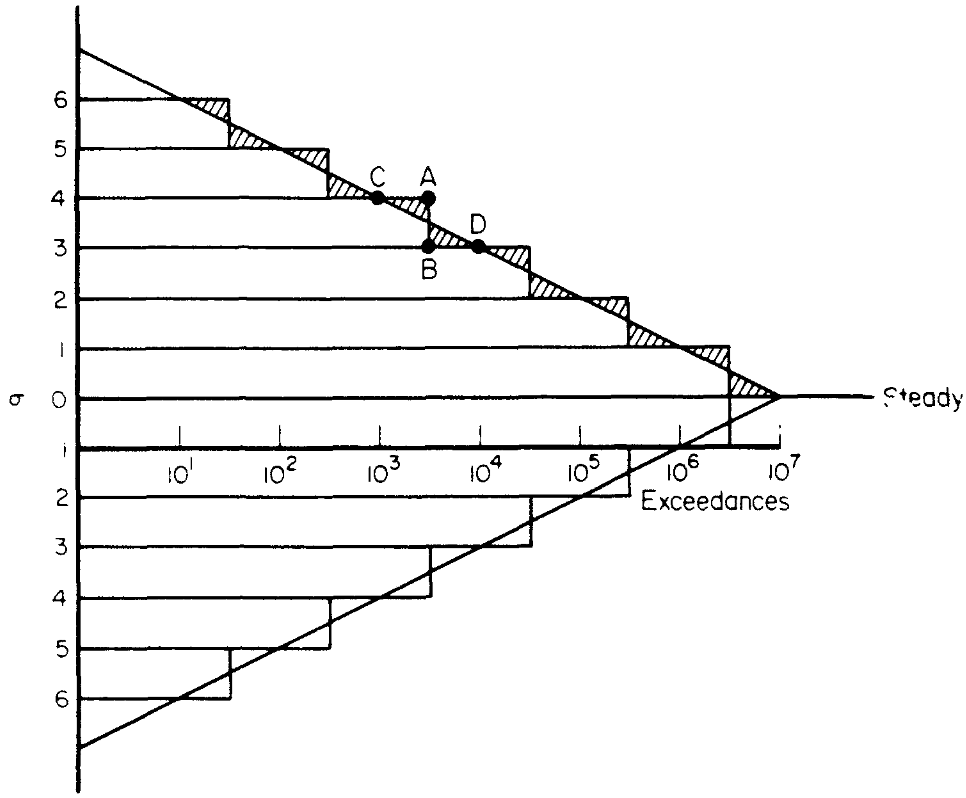

Example of level approximation (only 6 levels shown for clarity)

Level	Exceedances
6-6	30
5-5	300
4-4	3000
3-3	30000
2-2	300000
1-1	3000000

FIGURE 11. OBTAINING STRESS LEVELS AND EXCEEDANCES

In reconstituting a stress history the exceedance diagram is always idealized by a number of discrete levels. Considering too many stress levels is impractical and ignores the fact that the spectrum is a statistical representation of *past* experience and that the analysis is a prediction of the *future*. Accounting for too many stress levels would be presuming that stresses can be predicted to occur in the future exactly as they have in the past, which they will not. The discrete levels do not have to be evenly spaced, but they usually are. Experience shows that 10 to 12 levels (each positive and negative) are sufficient for the desired accuracy; use of more than 12 levels does not significantly change the results. This can be appreciated from the fatigue crack growth analyses for one particular exceedance diagram, shown in Figure 12. The calculated life remains essentially the same once the number of levels is [illegible] 10).

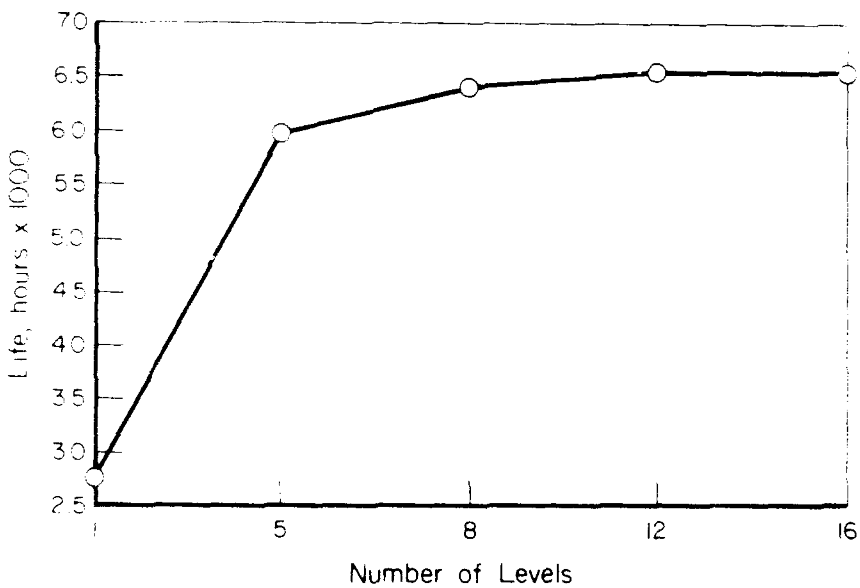

FIGURE 12. EFFECT OF LEVELS IN EXCEEDANCE DIAGRAM APPROXIMATION: COMPUTED NUMBER OF HOURS FOR CRACK GROWTH AS A FUNCTION OF NUMBER OF LEVELS. ONE LEVEL IS CONSTANT AMPLITUDE

For clarity only 6 levels (6 positive and 6 negative) are shown in the example in Figure 11. At each level a line is drawn intersecting the exceedance curve. Steps are completed by vertical lines (such as AB) in a manner that the shaded areas shown in Figure 11 are equal. Figure 11 also shows how the exceedances, and from these the number of occurrences of each level, are obtained.

Positive and negative excursions still have to be combined to create stress cycles. One might be tempted to select positive and negative excursions in random combinations, as is done in TWIST. For the purpose of tests; however, when this is done for analysis a rainflow counting of the history will again be necessary to determine the stress ranges. This is a legitimate approach, but a simpler procedure can be employed. Since the spectrum was developed from a counted history in the first place, it should not be necessary to disarrange it, and then count it again. Basically, the result is known a-priori. The result of counting will generally be that the largest positive peak will be combined with the lowest valley. Foreseeing this, it is reasonable to combine positive and negative excursions of equal frequency. Stress ranges so established can be applied (semi-) randomly, as they are *already* pre-counted and interpreted. This leads to the largest possible load cycles (conservative), and the computer code does not need a counting routine. It is also *realistic*, because air is a continuous medium, and a down-gust must soon be followed by an up-gust of approximately equal magnitude (Figure 13).

4.2 Different Flight Types

The content of the stress history is now known, but the sequence must still be determined. If retardation is not an issue, sequencing of stresses is irrelevant. If load interaction must be considered, stress sequencing becomes of eminent importance. In many analyses the loads are applied in random order. However, with retardation, a *random* sequence *does not provide correct answers* when actual service loading is semi-random. A commercial aircraft experiences many smooth flights and occasionally a rough flight. This means that the loading is not truly random, but clusters of high loads do occur (Figure 14). Were these high loads (e.g. A, B, and C in Figure 14a) distributed randomly as in Figure 14b, as is usually done in analyses, they would each cause retardation. Because of the clustering, the retardation will be much less (in Figure 14a, only A will cause retardation, B & C are overshadowed by A). Realistically then, fatigue crack initiation and growth analyses must principally account for a mixture of flights of different severity. This is defined as

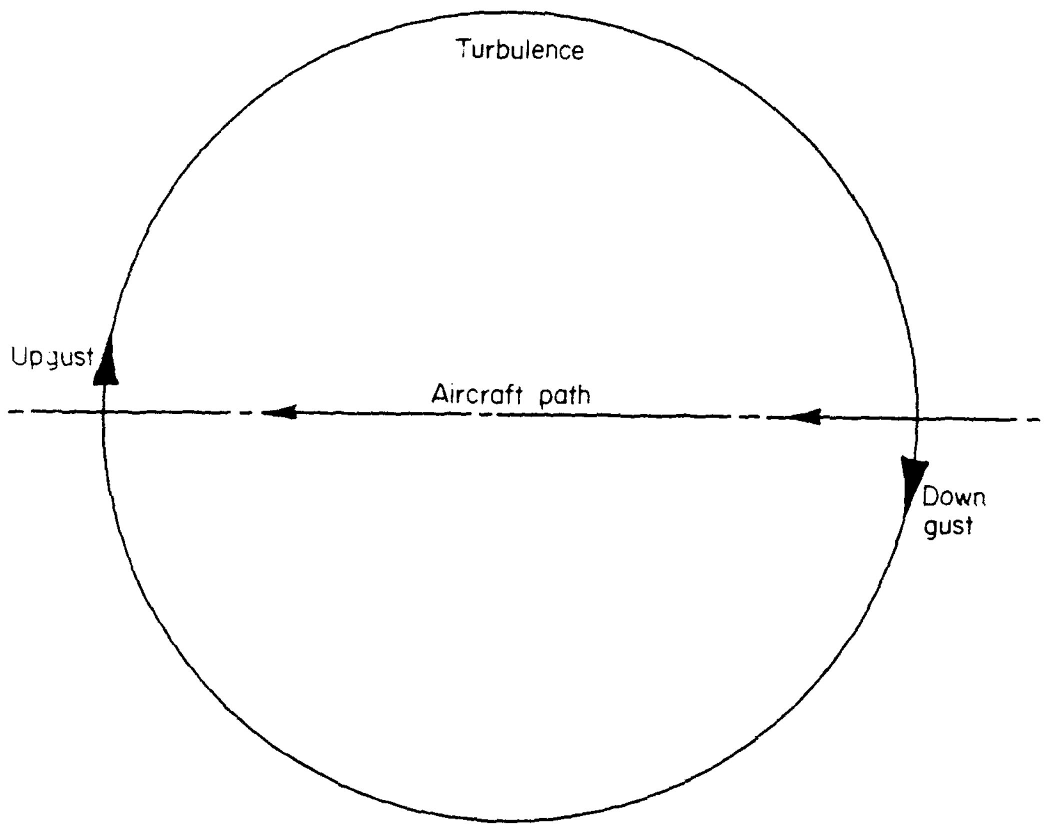

FIGURE 13. TURBULENCE, GUSTS, AND CONTINUITY OF AIR UP AND DOWN GUST OF ABOUT EQUAL MAGNITUDE OCCUR IN CLOSE SUCCESSION

semi-random loading. There will be fewer severe flights than mild flights, as shown in the example Figure 14. In the computer analysis *flights* of different severity must be applied in random sequence, and the cycles within each flight must be random. Such a semi-random sequence can be developed in many ways. A simple algorithm is shown in Table 2 on the basis of Figure 15. Mild and severe flights are constructed by recognizing that the exceedance diagrams for the individual flights are of the same shape, as demonstrated by Bullen [6], but with different slopes as shown in Figure 15c, their total making up the diagram of total exceedances (Figure 15a). The following example is based upon a schematic exceedance diagram for 100 flights; again only 6 levels are used.

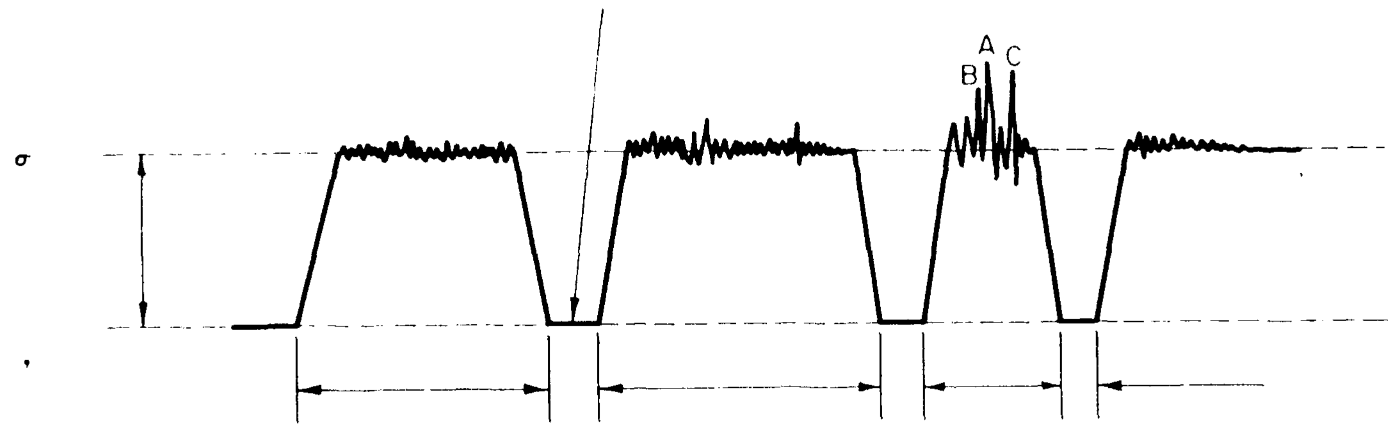

(a) Truly Semi-random (Real Situation)

(b) Random (Commonly done, but very wrong if there is retardation).

FIGURE 14. REAL (SEMI-RANDOM) AND WRONG (RANDOM) HISTORIES

TABLE 2. GENERATION OF STRESS HISTORY WITH DIFFERENT PERIODS BASED ON FIGURE 15

1	2	3	4	5	6 3 x 5	7 3 - 6	8	9	10 12 x 9	11 6 - 10
Level	Exceed-ances Fig. 15a	Occurrences	Type A exceed. Fig. 15b	Occur in A	Occur in 3 types A	Remainder	Type B exceed. Fig. 15c	Occur in B	Occur in 12 types B	Remainder
6	3	3	1	1	3	–	–	–	–	–
5	21	18	3	2	6	12	1	1	12	–
4	132	111	12	9	27	84	5	4	48	36
3	830	698	48	36	108	590	20	15	180	4110
2	5750	4920	158	110	330	4590	100	80	960	3630
1	43650	37900	575	417	1251	36649	480	380	4560	32089
			Total number of periods						12 + 3 = 15	

12	13	14 36 x 13	15 11 - 14	16 15/49	17 16 x 49	18 15 - 17	19 18/12	20 9 + 19	21	22
Type C exceed. Fig. 15c	Occur in C	Occur in 36 types C	Remainder for 49 type D	Occur in type D	Occur in 49 types D	Remains	Distributed in 12 type B	New type B	Exceed. of D	According to diagram Fig. 15c
–	–	–	–	–	–	–	–	–	–	–
–	–	–	–	–	–	–	–	1	–	–
1	1	36	–	–	–	–	–	4	–	–
8	7	252	158	3	147	11	1	16	3	1
52	44	1584	2046	42	2058	-12	-1	79	45	20
400	348	12528	19561	399	19551	10	1	381	444	300
		15 + 36 = 51			51 + 49 = 100					

Same for negative levels if applicable. Periods: 3A + 12B + 36C + 49D = 100 total.

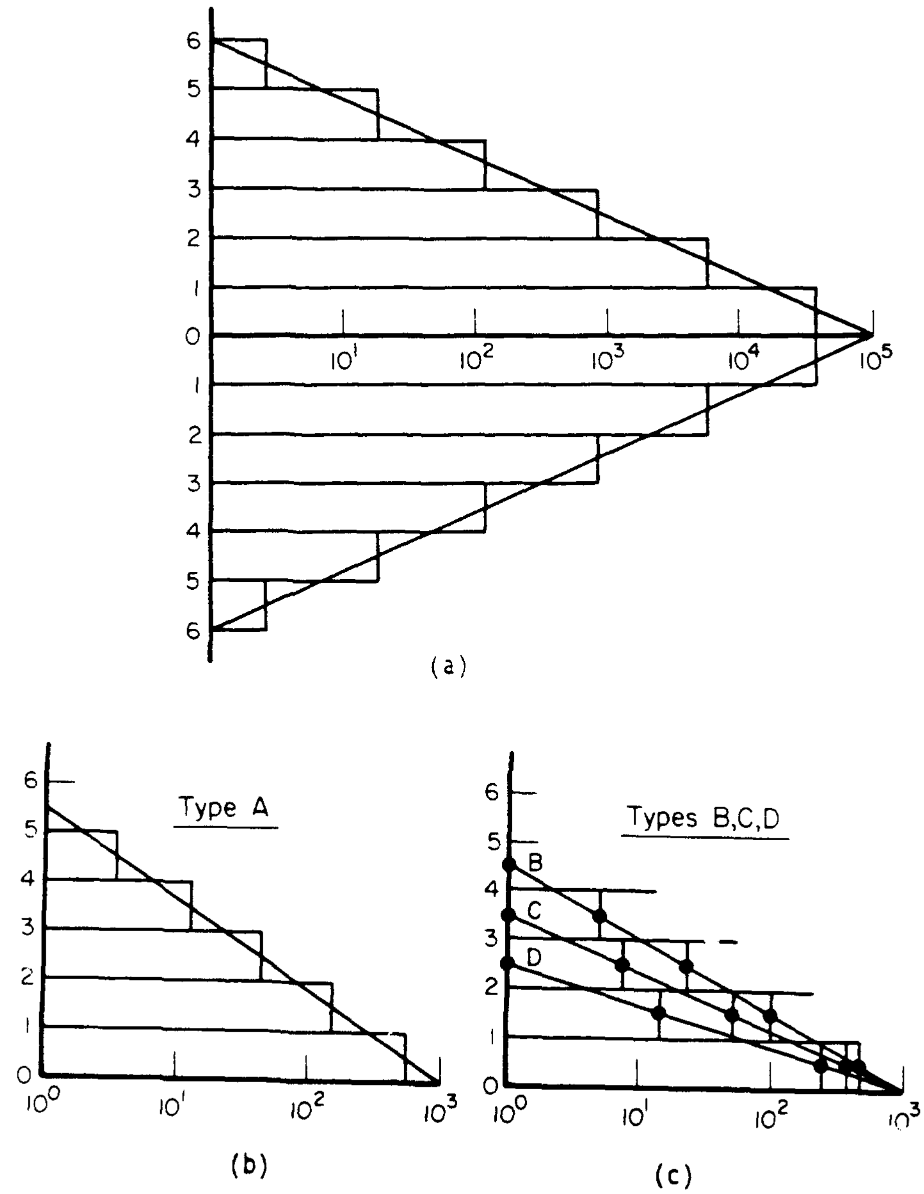

FIGURE 15. STRESS HISTORY WITH DIFFERENT FLIGHTS (SEMI RANDOM)

The different flights are constructed as illustrated. The total number of exceedances is 100,000, so that the average number of exceedances per flight is 100,000/100 = 1,000 [6]. This provides the end-point in Figures 15b and 15c. The highest level occurs 3 times (Figure 15 and Table 2, Column 3). Naturally, it will occur only in the most severe flight denoted as A. Letting this level occur once in A, the exceedance diagram for A is established as shown in

Figure 15b, because the highest level (6) provides the point of 1 exceedance. Flight A can occur only three times, because then the cycles of Level 6 are exhausted. The exceedances for A are read from the exceedance diagram of A (Figure 15b), and from these the occurrences (number of cycles) are determined as in Columns 4 and 5 of Table 2. There being three Type A flights, the total cycles for all A flights are shown in Column 6. These cycles are subtracted from the total so that the remainder for the other 97 flights is as shown in Column 7.

The next most severe flight is Type B. Its highest level will be Level 5, which will occur once. This information permits construction of the exceedance diagram for B as shown in Figure 15c, Level 5 being at 1 exceedance. The exceedances and occurrences are determined as in Columns 8 and 9 in Figure 15. Since there were only 12 cycles of Level 5 left after subtraction of three flights A (Column 7), there can be 12 Type B flights. These 12 flights will use the number of cycles shown in Column 10, which must be subtracted from those in Column 7 to leave the remaining cycles in Column 11.

Flight C is constructed in the same manner. There can be 36 Type C severity flights and then the cycles of Level 4 are exhausted. One could go on in this manner, but since there now are only 49 flights left, it is better to divide the remaining cycles in Column 15 by 49 in order to distribute them evenly over 49 Type D flights. This is done in Columns 15-17. There are some cycles unaccounted for, and a few too many cycles were used as shown in Column 18. These are of lower magnitude, contributing little to crack initiation or growth – and since the diagram is only a statistical average – this little discrepancy could be left as is. However, if one wants to be precise, they could be accounted for by a little change in the content of Flight C, as shown in Columns 18-20.

If more than 6 levels are used, more (and different) types of flights can be generated. However, this was an example only, and there is no need to go to extremes as long as a semi-random history is obtained, recognizing that flights of different severity do occur and that the higher loads are clustered in those flights. No matter how refined the procedure, the actual load sequence in practice will be different. In accordance with the nature of the loading, there are only three Type A flights of a high severity in the total of 100. The majority consists of mild flights of Types D (49) and C (36). Regardless of the number of levels chosen and the number of flights, the above procedure will reflect this reality. Other procedures can be devised, but the above is a rational one and easy to implement [4].

In crack initiation and growth analyses the various flights must be applied in random order and the cycles within each flight applied randomly. Thus, the second occurrence of any flight type will have a different sequence than its first occurrence, but the total cycle content will be the same. If the 'basket' with 100 flights is empty, it is 'refilled', and the process started anew; yet because of the randomization the flights and the cycles within each flight will appear in different order.

4.3 Issues of Importance

The stress history generated in the manner discussed provides the most realistic results when the total exceedances are on the order of 2,000 to 100,000 and the number of flights on the order of 50 to 1000. Therefore, it may be advantageous to reduce exceedance diagrams for smaller or larger numbers to the above ranges, as was done in Figure 10.

There are only a few issues of importance in the generation of a stress history, namely:

a. Flights of different severity must be applied. Random application of stresses derived by complicated means will negate all the efforts.

b. Deterministic loads must be applied at the point where they occur: GAG cycles must occur *between* flights; *random* application may defy all other sophisticated procedures.

c. A reasonable number of stress levels (10-16 positive and negative) must be selected. More levels will complicate the procedure without improving the results and make the generation of different flight types much more cumbersome.

d. Positive and negative excursions of equal frequency must be combined. Random combinations will require subsequent counting, the result of which can be foreseen, while the stress history was based on an already counted history in the first place.

e. The total number of flights and cycles must be in accordance with the total exceedance diagram.

The above criteria account for what may be called the *signature* of the loading. Small changes in these, including clipping [1,4,5], will usually have more effect on crack initiation and growth than any complicated means of establishing stress levels.

It is important to emphasize that the TWIST spectrum is based on measurements and used for demonstration in this report; it should be compared with spectra furnished by the OEM. Another important data source is the NASA/DOT/FAA aircraft loadings data [2]. In developing a stress history for a given repair in an aircraft fuselage, the repair engineer may be well advised to compare the stress history he or she develops with the proposed history and to use the most severe of the two.

5. FUSELAGE STRESSES

5.1 Scope

The basic spectrum and stress history have now been established. What still needs to be done is adjustment of the stress axis (actual stress) for the fuselage. There are two relatively simple ways to accomplish this:

a. Approximate fuselage stress analysis

b. Limit load analysis.

These two possibilities are discussed in the following sub-sections.

5.2 Approximate Fuselage Stress Analysis

Figure 16 shows an aircraft's weight distribution. Only the *fuselage* weight is of importance for fuselage bending; it is assumed to be evenly distributed. As shown in Figure 17, local bending moments due to vertical gusts are determined from static equilibrium requirements. Given the Station No., x, of the repair, which is always known, the moments (M_F and M_t) are determined, and from this the approximate stresses can be readily calculated as shown in Figure 18.

Circumferential stresses can be calculated as follows:

$$\sigma_p = \frac{pR}{t} \quad .$$

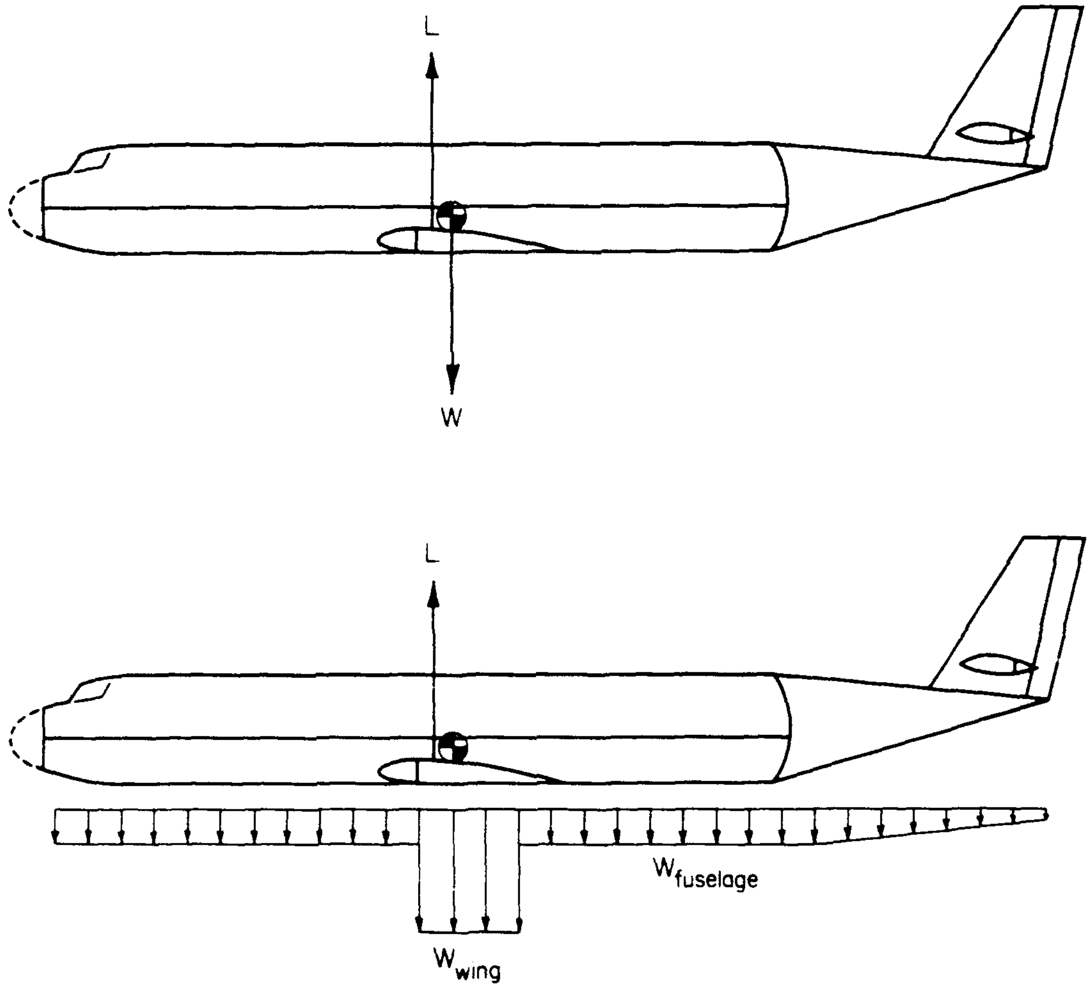

FIGURE 16. FUSELAGE LOADING

This pressurization stress cycle occurs once per flight. The circumferential stresses are generally reduced by approximately 20 percent near frames and 10 percent near tear straps. Longitudinal stresses are due to pressurization, σ_{pl}, and bending at the 1 g load (L - W), $\sigma_{b1\text{-}g}$. The pressurization stress is:

$$\sigma_{pl} = \frac{p\pi R^2}{2\pi Rt + k\ A_{st}} \tag{5}$$

where

- k = number of stringers
- kA_{st} = $\alpha_1\ 2\ \pi$ Rt and $\alpha_1 \approx 0.8$ (based upon a typical stiffening ratio of 0.4, but can be determined for each aircraft type).

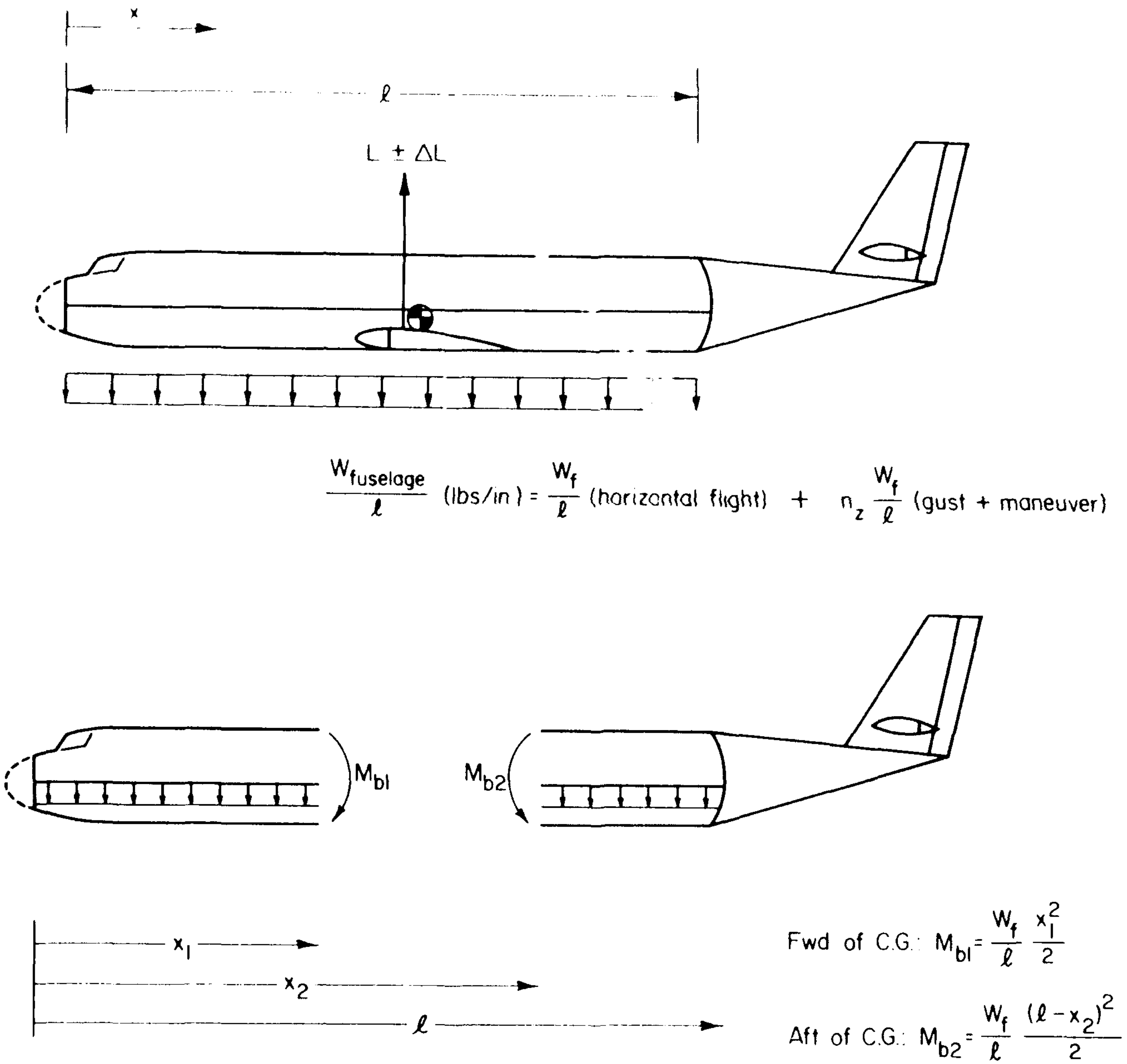

FIGURE 17. FUSELAGE BENDING

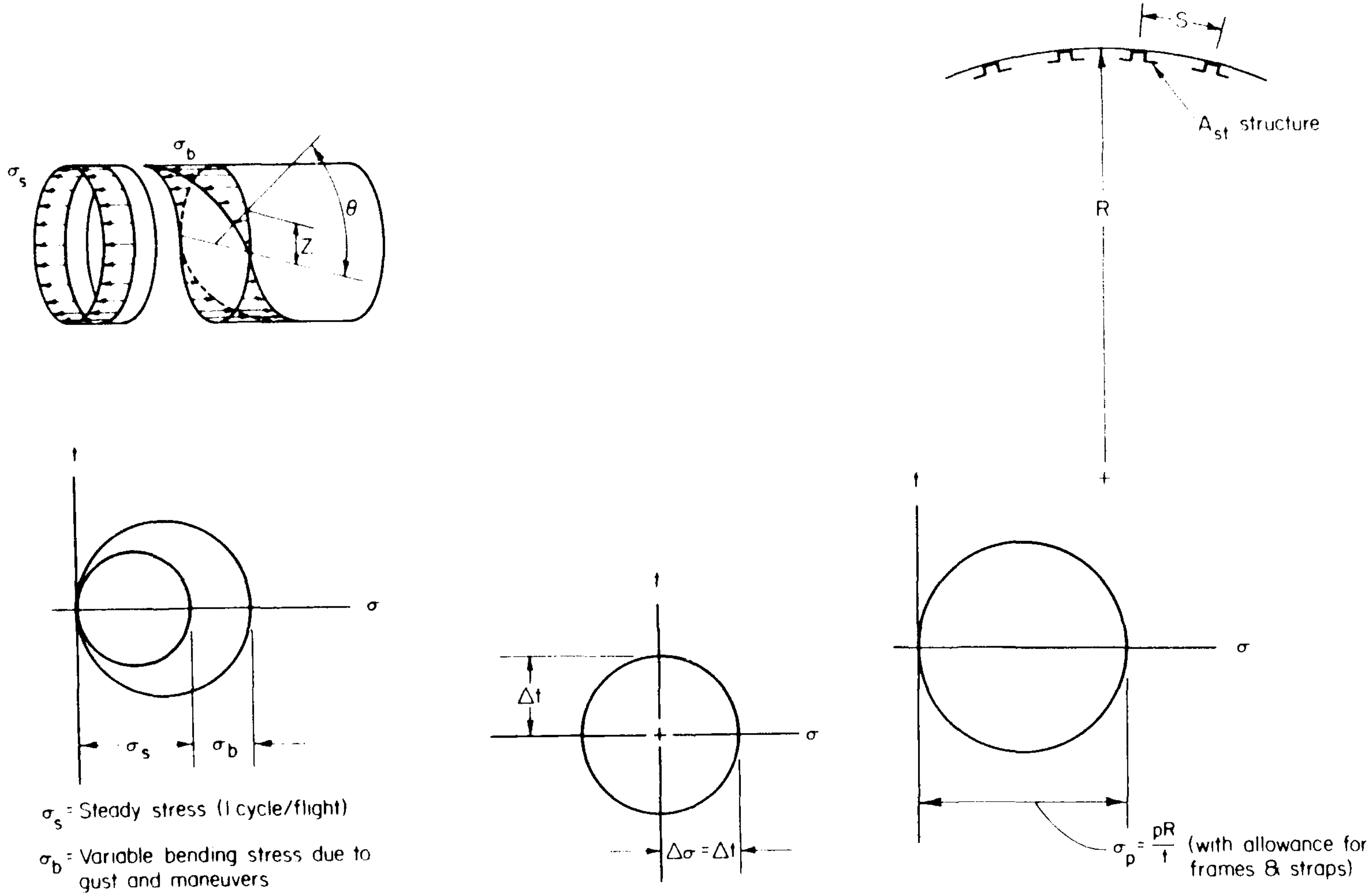

a. Longitudinal

b. Torsion – variable amplitude stress due to lateral gust and maneuvers

c. Pressurization and longitudinal cracks: steady stress part (1 cycle per flight)

FIGURE [illegible]. FUSELAGE STRESSES

This leads to:

$$\sigma_{pl} = \frac{p\pi R^2}{2\pi Rt(1 + \alpha)} \approx \frac{p\pi R^2}{2\pi Rt(1 + 0.8)} = \frac{p}{3.6Rt} \quad . \tag{6}$$

The bending stress is:

$$\sigma_{bl} = \frac{M_b Z}{\pi R^3 t + \frac{k}{2} A_{st} R^2} = \frac{M_b R \sin\theta}{\pi R^3 t + \alpha \pi RtR^2} \approx \frac{M_b \sin\theta}{1.8\pi R^2 t} \quad . \tag{7}$$

The total stress at 1-g loading, σ_l, is then

$$\sigma_l = \sigma_{pl} + \sigma_{bl} \tag{8}$$

where σ_{bl} is the bending stress from Equation (7) for the 1-g bending moment. Superposed on this 1-g stress is the cyclic bending stress due to inertia during gust and maneuvers.

The spectrum (Figure 8) shows that the once per 600 hours stress excursion (at 100 exceedances in 60,000 hours) is 1.3 times the "steady" stress, which in this case is the 1-g bending stress. Calculation of the 1-g bending stress therefore defines the entire exceedance diagram of Figure 10 in terms of real stresses.

The stress history can then be generated in accordance with the procedure described. Every cycle will be an excursion due to bending from the 1-g steady stress $\sigma_{b1\text{-}g}$; so that the stress history is described as:

$$\sigma_l(\text{time}) = (\sigma_{pl} + \sigma_{bl})_{\text{constant}} + \Delta\sigma_{bl}(\text{time}) \tag{9}$$

where

$\Delta\sigma_{bl}$ reaches $\pm$ 1.3 ($\sigma_{b1\text{-}g}$) once in 600 flights, as shown below:

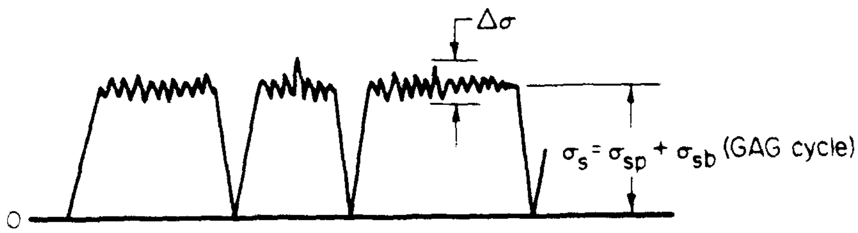

If necessary the shear stresses due to torsion and bending can be included.

$$\Delta\tau_t = \frac{\Delta M_t}{2\pi R^4 t} R = \frac{\Delta M_t}{2\pi R^3 t}; \; \Delta\sigma_t = \Delta\tau_t \quad . \tag{10}$$

With the other stresses already obtained, this permits calculation of the largest principal stress – the one to be used in the fatigue and crack growth analyses.

A complication that must be considered is that fuselage bending stresses due to wing gusts and torsional stresses (due to lateral gusts) vary independently. It is likely, however, that the torsion contribution will be small for circumferential cracks, and the bending contribution will be small for most longitudinal cracks.

Of course the value of α_1 in σ_{pl} in Equation (6) can be adjusted in a stress analysis program for different aircraft types. The effect of longitudinal stringers on bending stresses and longitudinal pressurization stress is properly accounted for. Some adjustments to the circumferential stresses to account for the effects of straps and frames must be made, and appropriate adjustments must be made for door and window cut-outs and framing.

When the stresses in the basic structure are known in this manner, the stresses in the repair can be calculated by compatible displacements (or other local stress analysis techniques) for any repair.

5.3 Limit Load Analysis

An alternative, but simplified, way to obtain the stress conversion it as follows:

> Limit load is basically the load that is expected to occur once in the aircraft life (i.e. once in 60,000 hours as shown in Figures 9 and 10). The structure is sized such that the stress at ultimate load is equal to the material's design allowable strength. The safety factor between ultimate and limit load is 1.5 (the airworthiness requirement). Hence, the limit load stress follows immediately as the design allowable stress divided by 1.5. One small limitation to this approach is that different manufacturers do use different allowables, and these allowables are often lower than the "true" statistical allowable of the material.

In any case, given the material and hence the design allowable stress, the limit load stress follows as above. Since this is the stress which is assumed to occur once in about 60,000 hours, the beginning points in Figures 9 and 10 are known, and hence the whole exceedance diagram can be estimated. Another rule of thumb to consider in this analysis is that limit load stresses (in 2024-T3) are usually set no higher than about 35 ksi.

As aircraft structures are seldom designed exactly to the design allowable limits (there is always a margin of safety, which varies from location to location), the disadvantage of this method is a loss in accuracy, but the accuracy may suffice for comparative analyses. Its advantage is that no special allowances have to be made for location and structural details. (The assumption being that the original structure was designed to conform to limit load margins).

6.0 COMPARISON OF PROPOSED STRESS HISTORY GENERATION SCHEME WITH MANUFACTURER'S

To provide an appreciation of how representative crack growth curves, as calculated with the proposed stress history and spectrum, compare with those calculated by manufacturers, a comparison was made of crack growth computations based upon the proposed procedure and those based on stress histories for the KC-135 and EC-135 [8]. The latter were kindly provided by the US Air Force. Only longitudinal stress estimates are considered in these examples.

The following discussion is based on the word "spectrum" meaning the total load experience (in terms of an exceedance diagram or otherwise), while the specific sequence of loads or stresses used in an analysis or test is called a "stress history". These definitions were adhered to in the previous part of this report, but in the general literature they are often confused or used alternatively without explanation. The two are essentially different — a stress history may be a very loose interpretation of the spectrum, as will be shown below. In practice the word "spectrum" is often used for both, which may lead to confusion.

Before presentation of the results of the comparison, the stress histories for the military versions of the B-707-720[8] require some discussion, because otherwise a fair comparison is not possible. The details of the analysis leading to the stress histories are not elaborated upon in Reference [8]. Therefore, only the results are reviewed briefly.

The fuselage of the aircraft is divided into Areas A through O, as shown in Figure 19. Stress histories for these areas were derived, and these were assumed to be valid throughout the area without regard to stress gradients or detail design. (It should be noted that the bottom of Figure 19 roughly represents the neutral axis for fuselage bending.) Each of these areas stress histories was derived on the basis of the load spectrum, taking into account flight conditions (point-in-the-sky approach accounting for different flight segments as discussed). Although details are not given, other evidence[9] shows that the manufacturer used a loose interpretation of TWIST (the spectrum proposed here) for the stress history in a recent full-scale fatigue test; it is therefore reasonable to assume that similar considerations were used in the derivation of the stress histories discussed here.

Apparently [8], stress histories for a variety of missions of the different military versions of the aircraft were derived. By means of crack growth calculations, details of which are not specified, one particular mission (identified as Mission 3) was determined to be the most severe. This led to a typical mission profile (stress history) as shown in Figure 20. Similar stress histories were developed for all areas specified, using only Mission 3 for all areas. The number of cycles in these missions, and the maximum stress in each area, are shown in Figure 19.

The first thing to be noted is that the most severe mission (which was taken as representative for all versions) pertains to the AWACS version. The radar disk above the fuselage may explain the fact that in Areas A through I the number of cycles is much larger than elsewhere and that the stresses do not follow the anticipated pattern. For this reason, Areas A through I could not be used for comparison with a commercial aircraft. This leaves Areas J through O, from which Areas J, K, and L were selected as the basis for comparison.

The cycle numbers per mission for these areas (Figure 19) do not seem to be consistent, as (one must assume that) the cyclic stresses are due to bending cycles, the number of which is the same for all areas in the fuselage. Be that as it may, Mission 3 includes 5 touch-and-go landings as illustrated in Figure 21. Because normal airline practice does not include touch-and-goes, the cycles concerned were eliminated. The stress histories for Areas J, K, and L are shown in Figure 22. It seems reasonable to assume that the cycles for the five touch-and-goes are as indicated. Eliminating these leads to the stress histories shown in Figure 22.

Note: Maximum stress in history, σ_{max}, and number of cycles in Mission 3, N, are shown

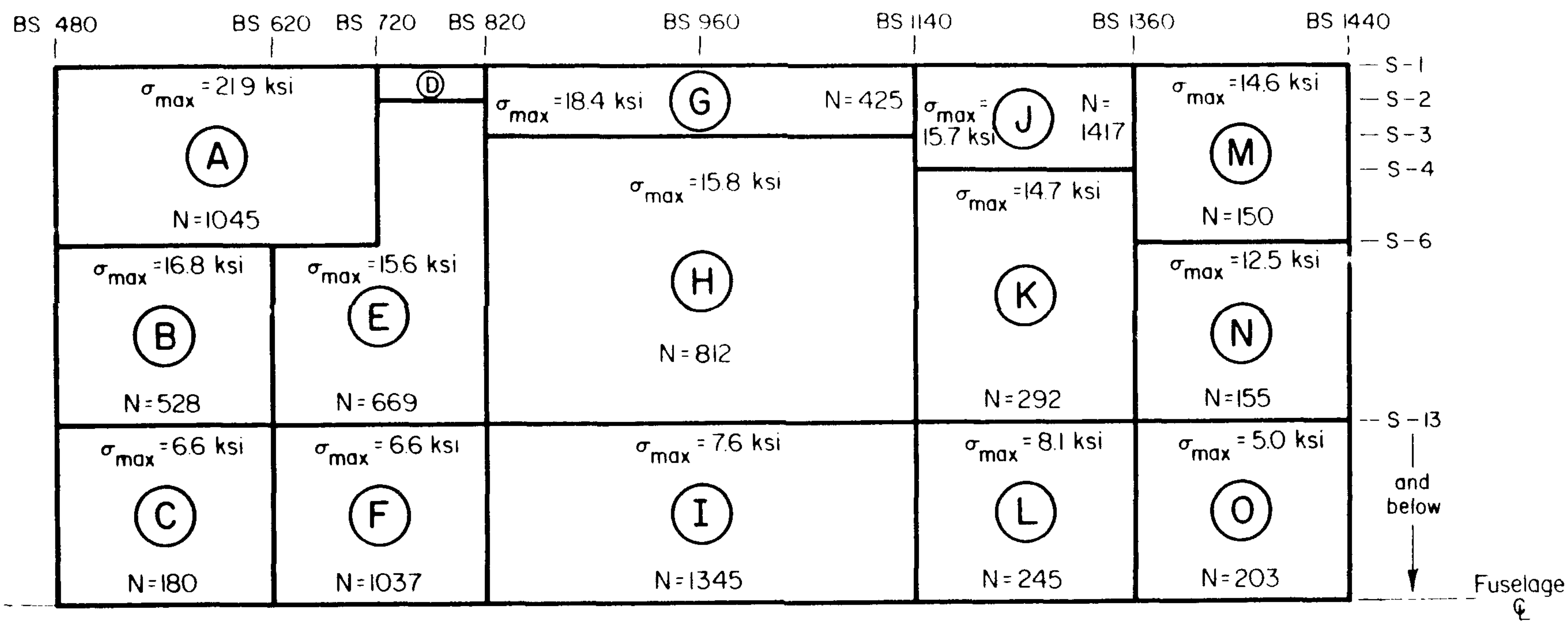

BS = Fuselage station
S = Stringer

FIGURE 19. AREAS OVER WHICH STRESSES ARE ASSUMED THE SAME

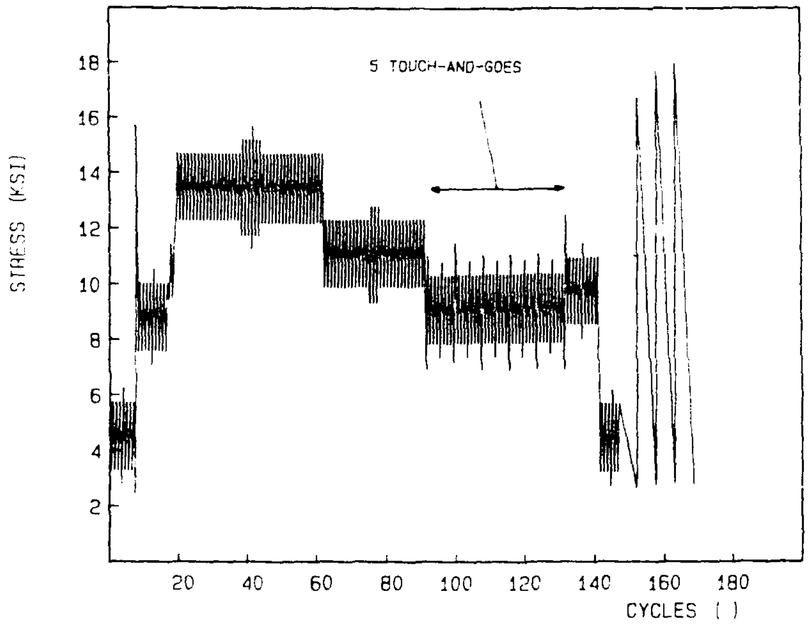

a. Area J

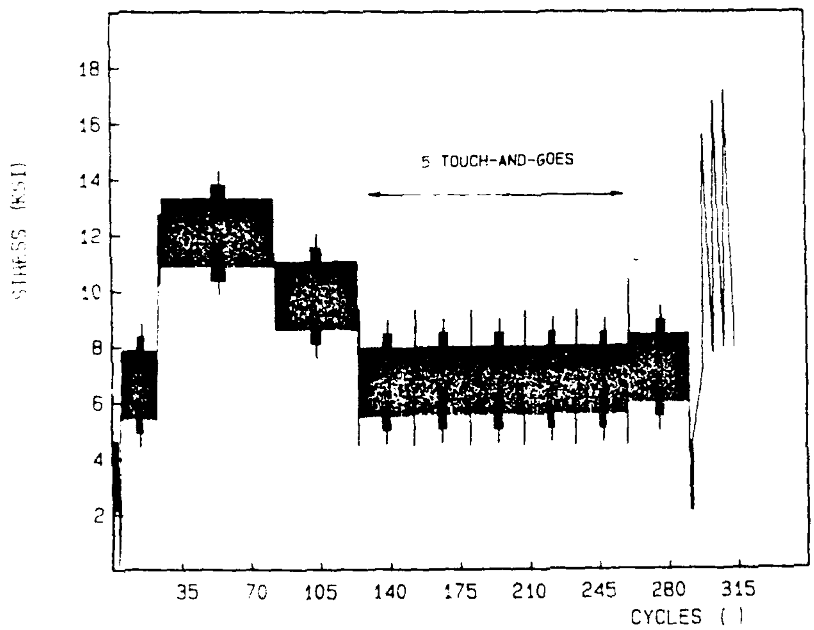

b. Area K

FIGURE 20. BOEING SPECTRUM; ALL FLIGHTS ARE THE SAME, LAST 3 CYCLES ARE MAKE UP CYCLES

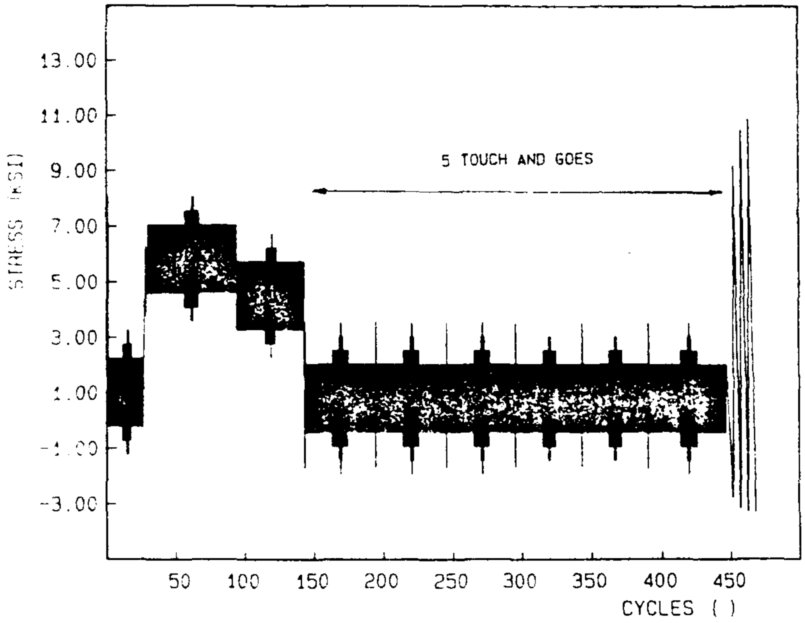

c. Boeing Spectrum for Area L

FIGURE 20. (Concluded)

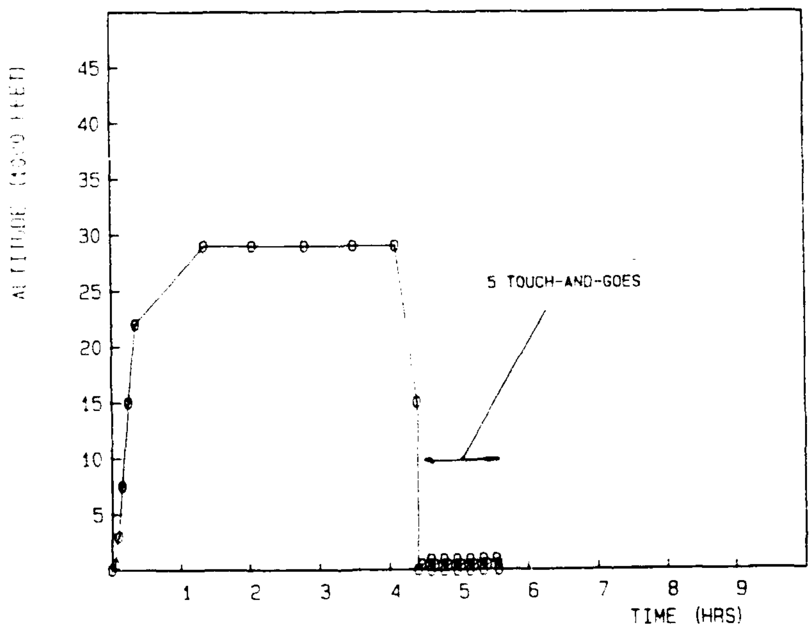

FIGURE 21. MISSION 3 ALTITUDE PROFILE

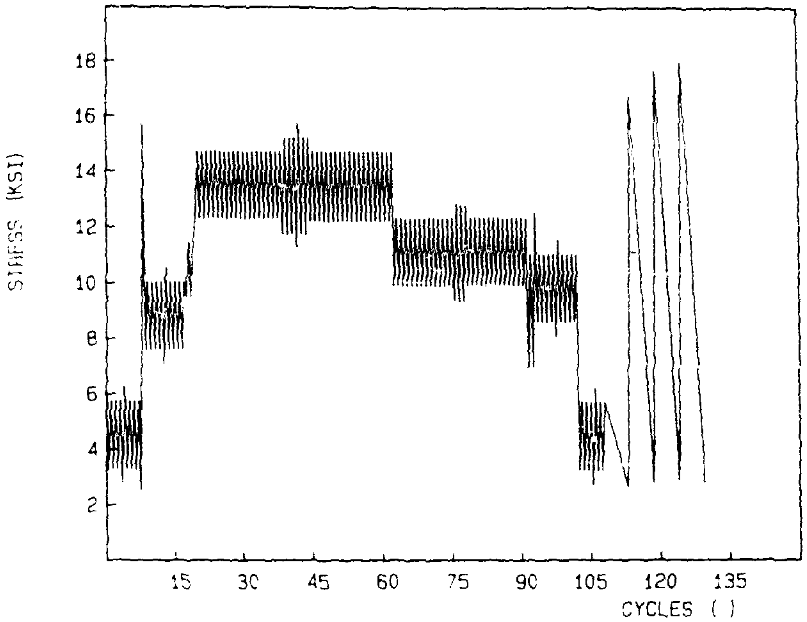

a. Area J

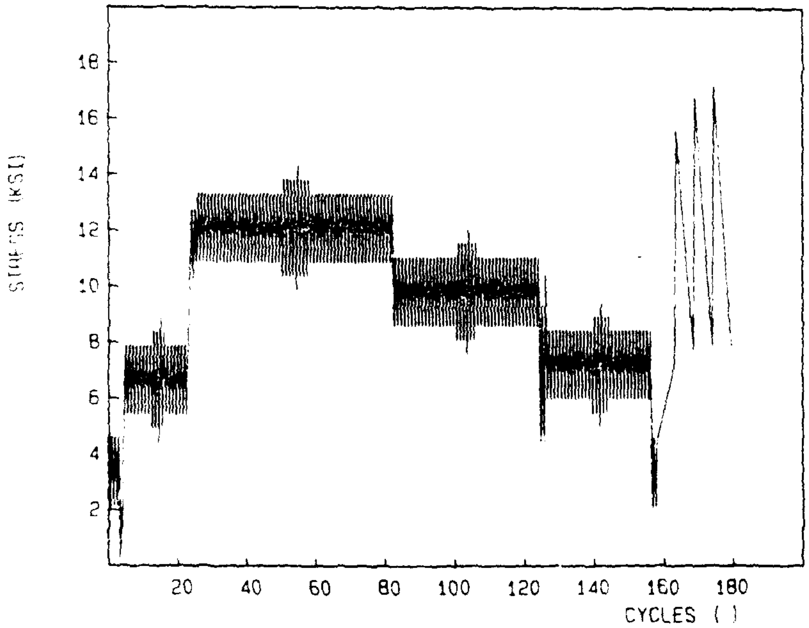

b. Area K

FIGURE 22. SHORTENED SPECTRUM, TOUCH AND GOES DELETED

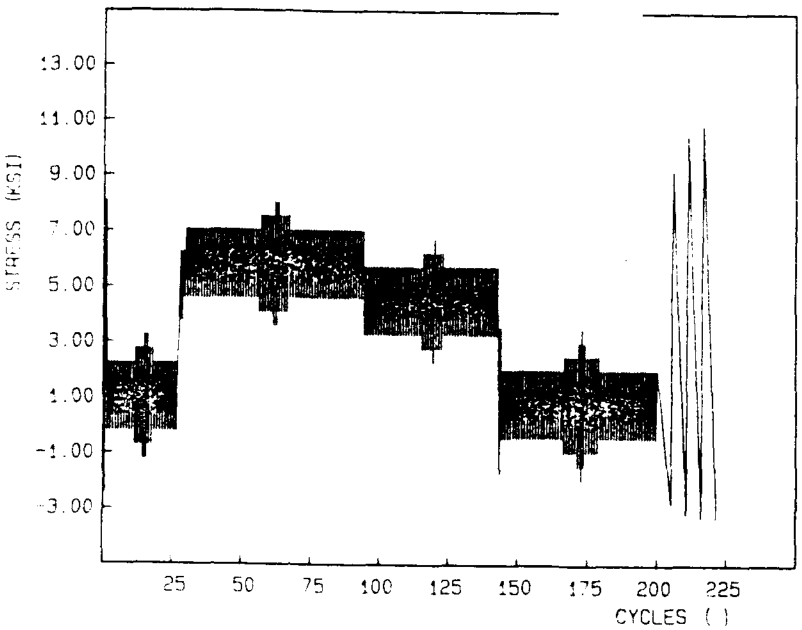

c. Area L

FIGURE 22. (Concluded)

The total number of cycles per mission (flight) is still inconsistent and remains unexplained. The stress histories in Figure 22 were considered representative for three areas over which the stresses vary appreciably. Also, the particular mission in the stress history is the only one: all flights are assumed to be equal. However, it should be noted that a small compensation is made for the fact that higher loads do occur from time to time. For this reason the last three cycles in all histories in Figures 20 and 22 are what is called in the industry "make-up cycles". The first of the three occurs once in every 10 flights, the second occurs once in every 100 flights, and the third occurs once in every 200 flights.

For a comparison with the stress histories proposed here the following conditions were considered:

- Maximum differential pressure of 9 psi
- Fuselage weight of 65,000 lbs (for the military version for which the comparison was made)
- The critical points covered by Areas J, K, and L are at the forward and top of these areas which are the worst, as the stresses will be decreasing from there.

The stresses were calculated for these conditions using the procedure in Section 5. From these the spectrum was obtained, and subsequently stress histories were determined, all in accordance with the procedures described in this report. The stress histories for Area J are shown in Figure 23. Note that there are five different types of flights. The stress histories for Areas K and L are similar, except that the stress values are different.

The objective of the computations was to show the effect of different methods of computing stress histories on predicted crack growth behavior. Therefore, the configuration and basic crack growth rate data used are immaterial, as long as the same situation and data are considered for both stress histories. Nevertheless, a configuration was chosen that is reasonably representative for aircraft structures, namely a through crack at a fastener hole (no load transfer), while the rate data were presented by a Walker equation with a coefficient of 3E-9, and exponents of 2 and 1, respectively.

The results of the computations for the three areas are shown in Figure 24. For Area J (the most critical for longitudinal stresses) the present history is conservative by a factor of two with regard to the manufacturer's history. For Area K they come out about the same, but for Area L the manufacturer's spectrum is far more conservative. Anticipated crack growth in the three areas according to the manufacturer's method of developing a stress history and according to the proposed method are shown in Figure 25. The proposed stress history would produce a much longer crack growth life in the area close to the neutral axis. This is reasonable, but rather insignificant, because inspection intervals would be based on the most critical area (Area J), where the proposed history is more conservative by a factor of two.

These relatively similar results must be considered with caution for the following reasons:

a. The manufacturer's stress history is the same in every flight; the proposed history recognizes that all flights are different.

b. The manufacturer's stress history recognizes that some load cycles occur at altitudes less that the cruising altitude, as shown in Figure 22, while the proposed histories implicitly assume that all cycles have the same mean stress. (It should be pointed out, however, that the cycles at lower mean stresses do not occur at a fixed mean either as assumed by the manufacturer.)

c. The manufacturer keeps the stresses the same over large areas, while the proposed history recognizes gradual stress gradients.

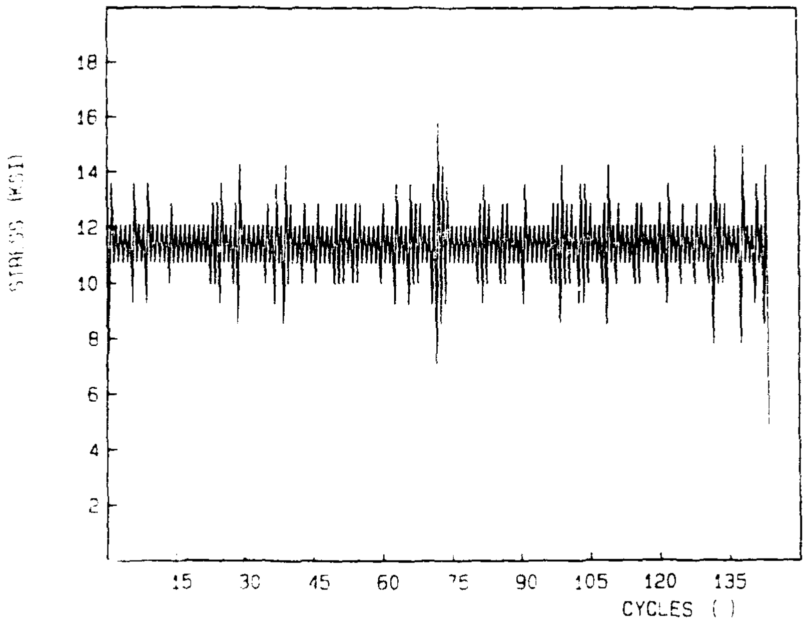

a. Flight Type 1 – Occurs 106 times in 133 flights

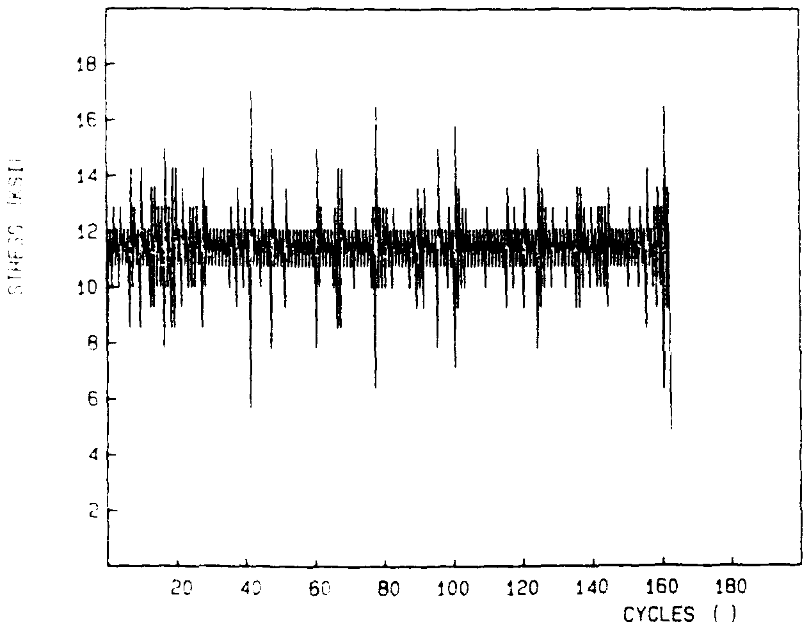

b. Flight Type 2 – Occurs 21 times in 133 flights

FIGURE 23. FLIGHT TYPES, EVERY OCCURRENCE WITH DIFFERENT SEQUENCE

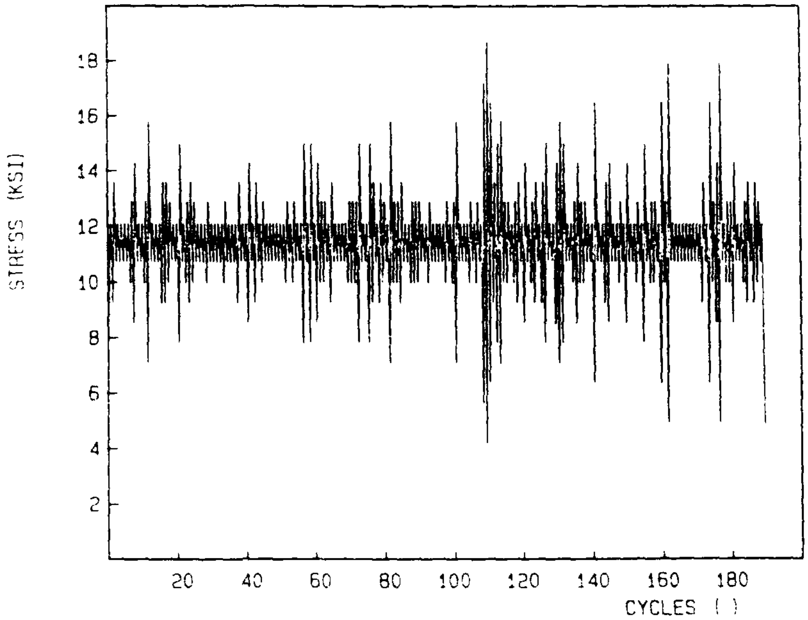

c. Flight type 3 - Occurs 4 times per 133 flights

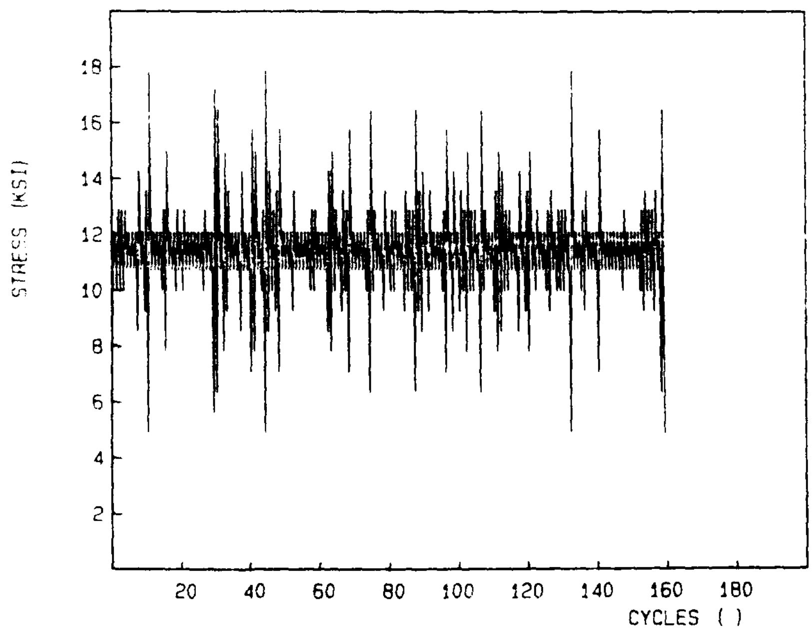

d. Flight Type 4 – Occurs once per 133 flights

FIGURE 23. Continued

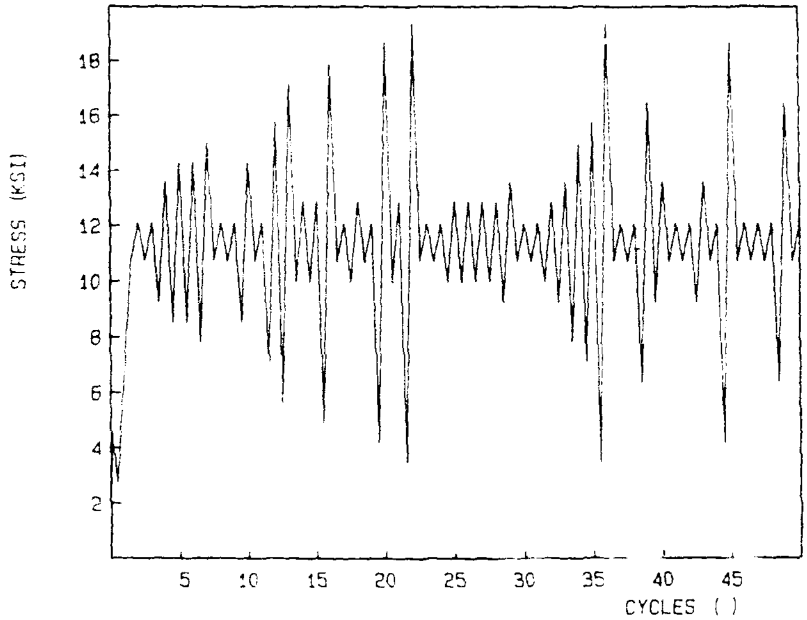

c. Flight Type 5 - Occurs once per 133 flights

FIGURE 23. Concluded

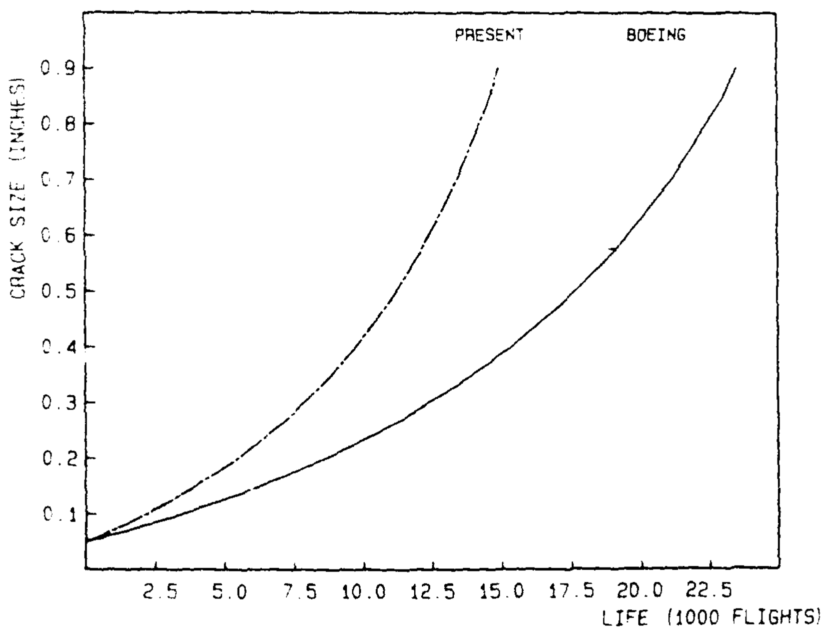

a. Run ID: 5742 – Area J

FIGURE 24. CRACK GROWTH COMPARISON OF BOEING AND PRESENT SPECTRUM

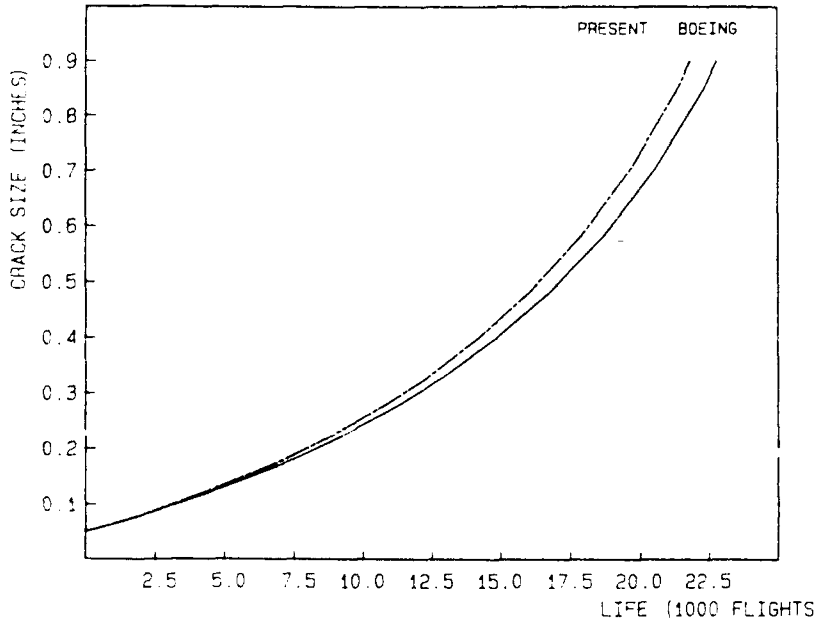

b. Run ID: 24657 – Area K

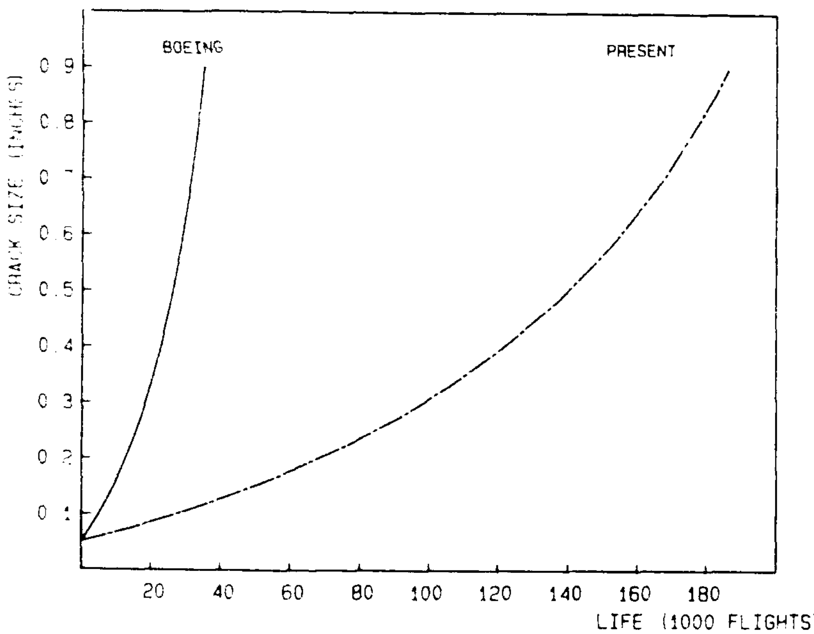

c. Run ID: 7387 – Area L

FIGURE 24. Concluded

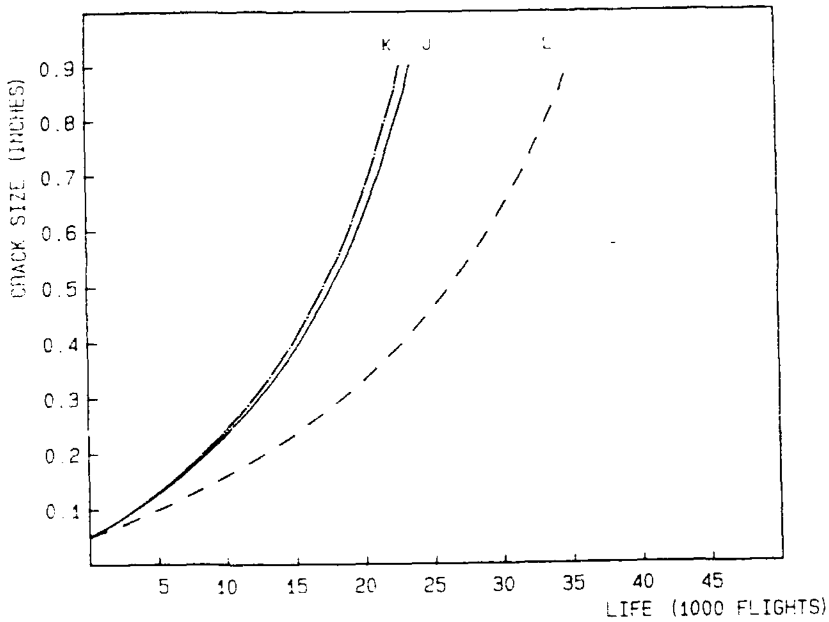

a. Run ID: 14835

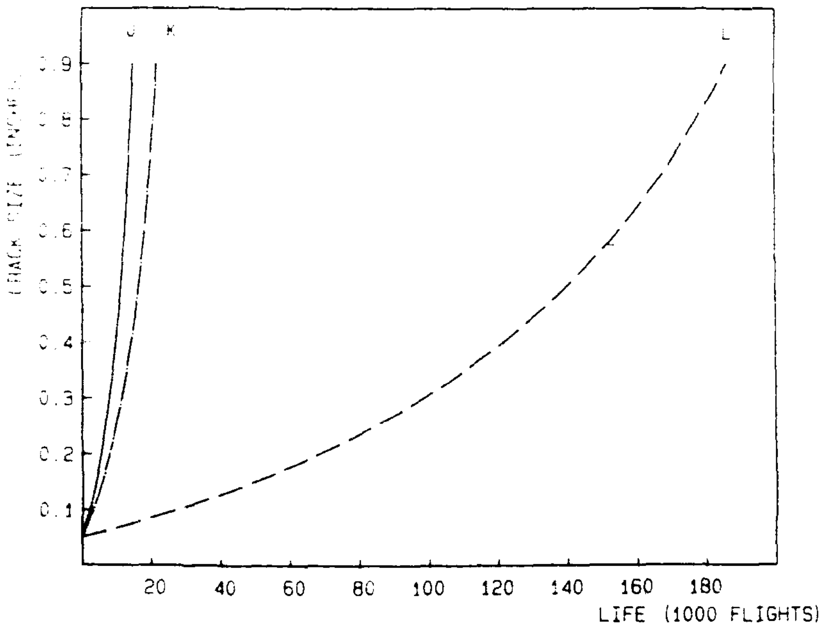

b. Run ID: 7387

FIGURE 25. CRACK GROWTH, PRESENT SPECTRUM FOR AREAS J, K, AND L

The stress history for Area J as shown in Figure 23 seems more representative of aircraft loading than the one shown in Figure 22a, despite the fact that Figure 22a reflects altitude differences. In reality the cycles at lower altitude (mean stress) are spread over different altitudes. The manufacturer assumes that they will occur at a fixed (lower) altitude, while the present procedure assumes them at a fixed higher altitude (conservative). In any case, the issue is of secondary importance, because it affects only the R-ratio. The effect can be assessed by estimating the relative number of cycles occurring at lower R; the result is that the effect is at most a factor of 1.3. Considering the simplifications in taking all flights to be the same in the history and by assuming this history is valid for large areas, the effect of R is probably inconsequential.

Both stress histories are based on numerous assumptions; the proposed history is based upon measurements, is conservative with regard to R-ratio effects, and is more realistic in accounting for different flight profiles. While the proposed method derives the stresses from generalization and simplification of the structure, the manufacturer's method does also, and results in essentially the same stress history.

REFERENCES

[1] Broek, D., The Practical Use of Fracture Mechanics, Kluwer Academic Publishers, 1988.

[2] Crabill, Norman L., The NASA Gigital VGH Program-Exploration of Methods and Final Results, Volume I-Development of Methods, Volume II-L 1011 Data 1978-1979: 1619 Hours, Volume III-B727 Data 1978-1980: 1765 Hours, Volume IV-B747 Data 1978-1980: 1689 Hours, Volume V- DC10 Data 1981-1982: 129 Hours, NASA Contractor Report 181909, NASW 4430, Eagle Engineering Inc., December 1989.

[3] De Jonge, J.B., et al., A Standardized Load Sequence for Flight Simulation Tests on Transport Aircraft Wing Structures (TWIST), LBF-FB-106, NLR TR 73029U, 1973.

[4] Schijve, J., The Analysis of Random Load-Time Histories With Relation to Fatigue Test and Life Calculations, Fatigue of Aircraft Structure, p. 115, Pergamon, 1963.

[5] Broek, D., and Smith, S.H., Fatigue Crack Growth Prediction Under Aircraft Spectrum Loading, *Engineering Fracture Mech.*, **11**, pp. 122-142, 1979.

[6] Bullen, N.I., The Chance of a Rough Flight, RAE TR 65039 (1965).

[7] Broek, D., Fracture Mechanics and Damage Tolerance Software, FractuREsearch Inc., 1987-90.

[8] Anon., Fuselage Load Spectrum for Modification Design Per Damage Tolerance Criteria, Enclosure to BMAC letter No.3-KC-135-6183-1130 to USAF.

[9] Fowler, K. R., and Watanabe, R. T., Development of Jet Transport Airframe Test Spectra, Boeing paper without date or number.